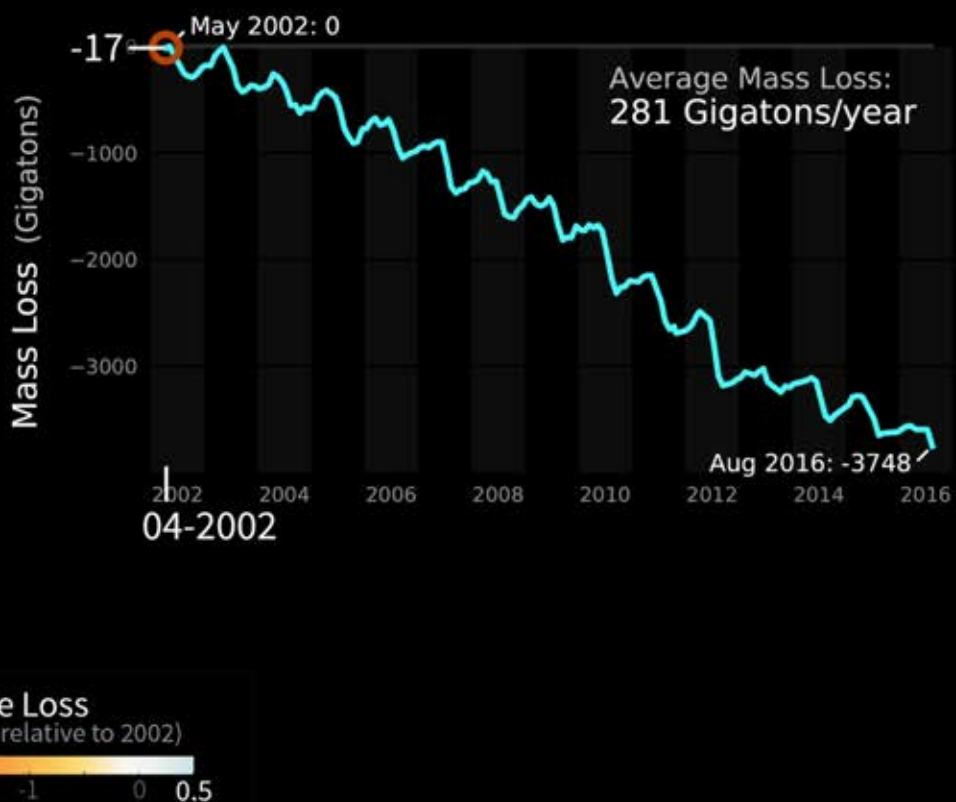




## GRACE Observations of Greenland Ice Mass Changes



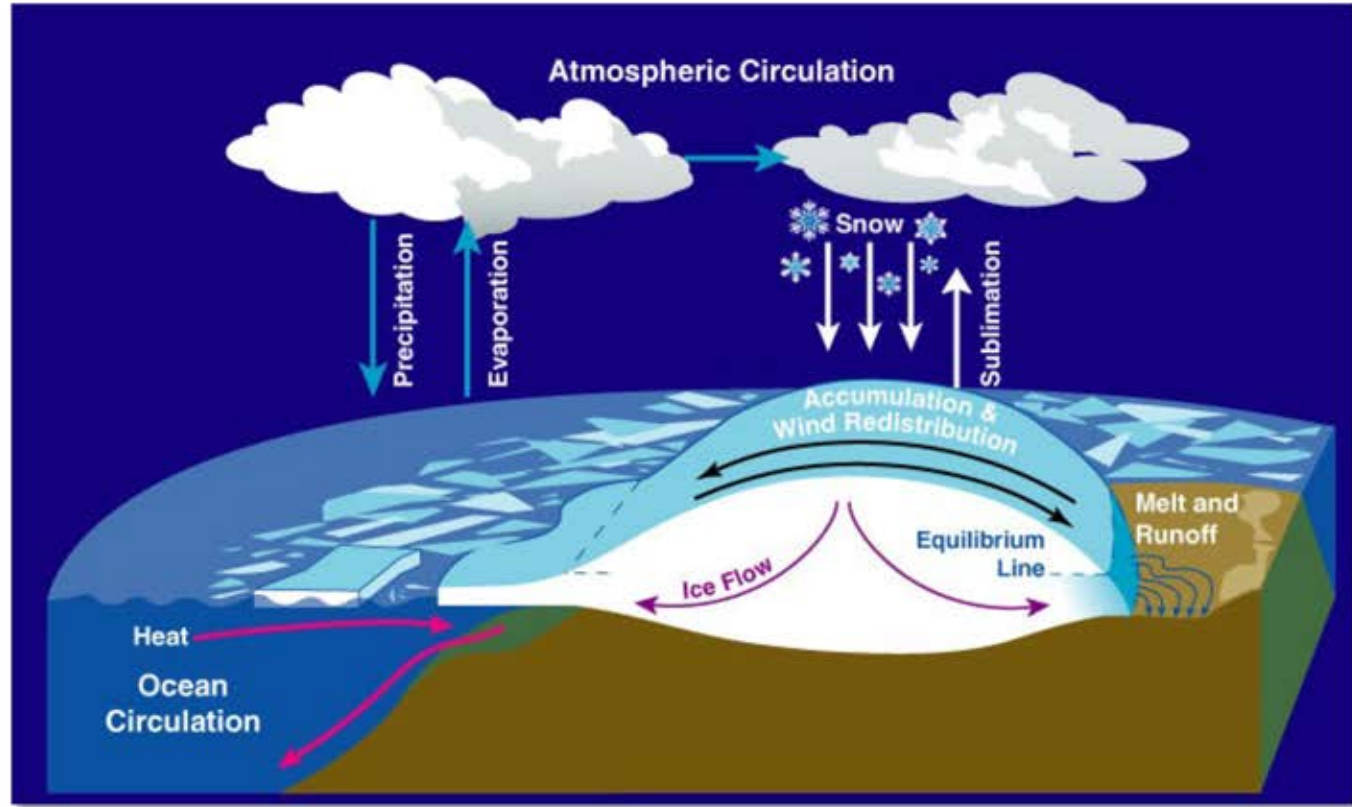
NASA, Sea level change, Observations from Space

## Observed Land Ice Changes

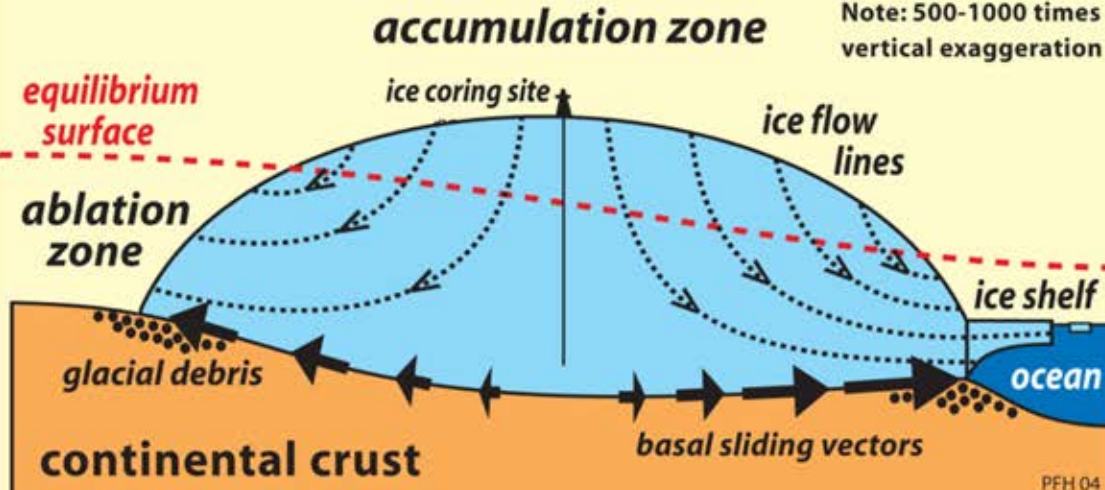
Csatho, Bea University at Buffalo, Buffalo, NY, USA

## Processes:

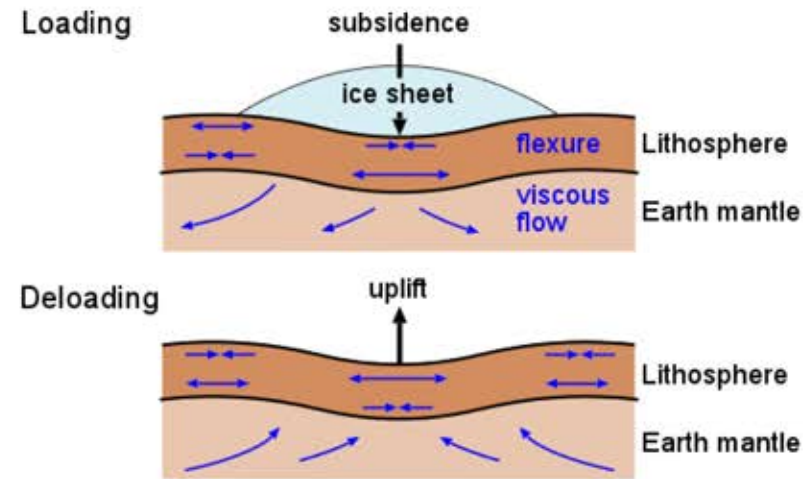
- Ice-atmosphere
- Ice-ocean
- Ice-solid earth
- Ice internal



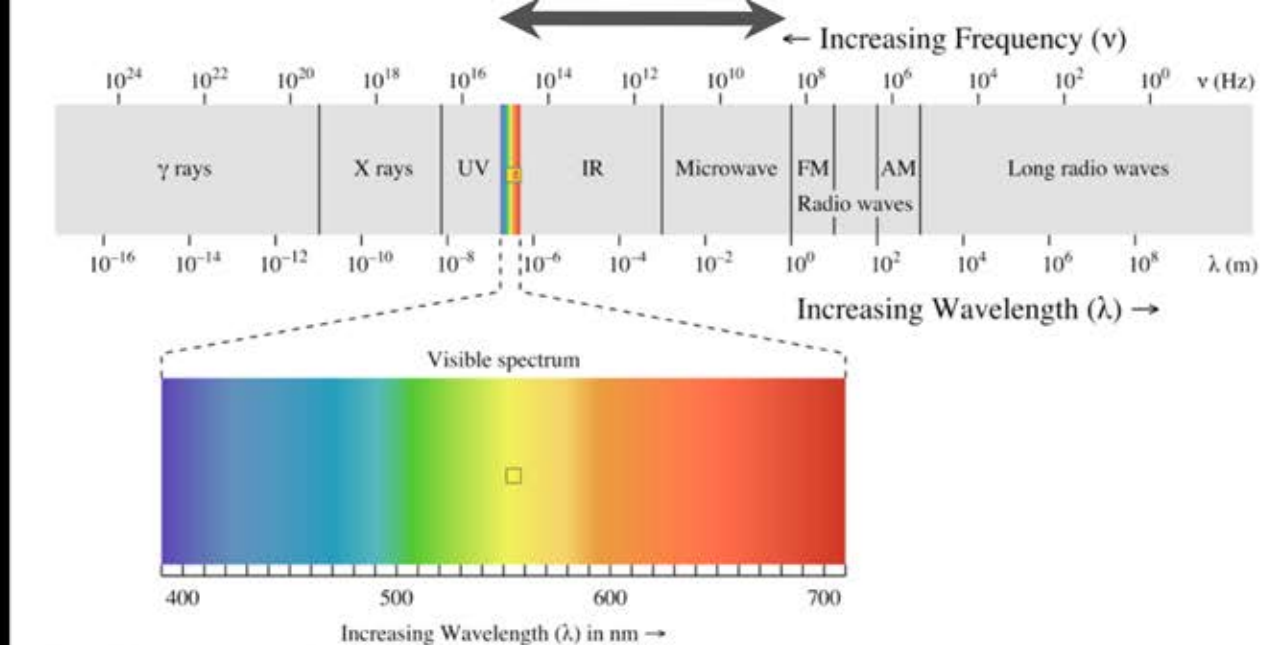
## IDEALIZED ICE-SHEET DYNAMICS



## Ice Solid Earth Interaction



# Observations NASA's fleet of satellites, 2015



Visible: Landsat 7/8

Microwave (passive): Scanning Multi-channel Microwave Radiometer (SMMR), Special Sensor Microwave/Imager (SSM/I)

Broadband: Clouds and the Earth's Radiant Energy System (CERES)

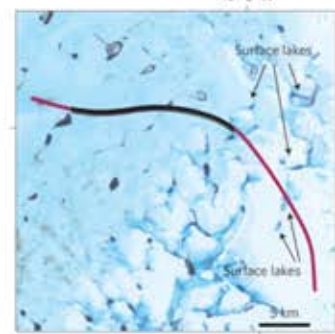
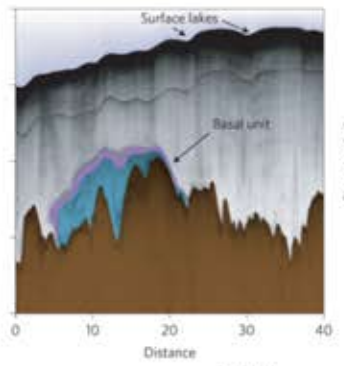
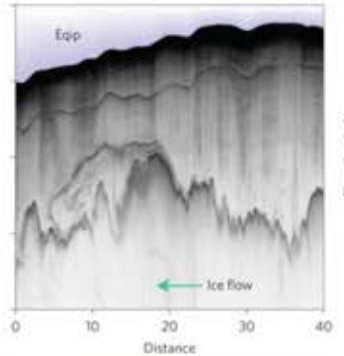
Laser (active): Ice, Cloud and land Elevation Satellite (ICESat)

Radar (InSAR): European Remote Satellite (ERS-1,2), RADARSAT-1,2

Gravity: Gravity Recovery and Climate Experiment (GRACE)

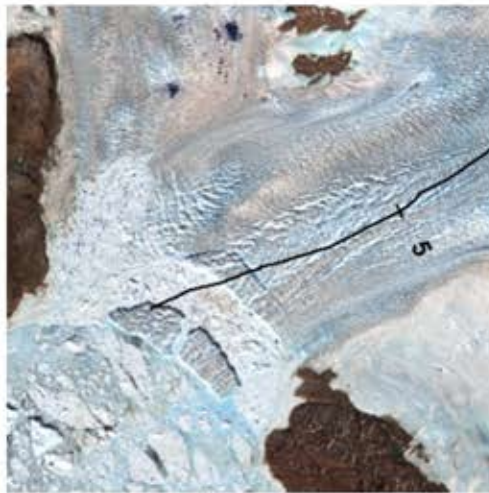
To characterize the state of land ice (ice sheets, ice caps and glaciers) and processes acting upon it, the geometry and properties of land ice surface, bed, ocean, atmosphere, etc. should be monitored

Ice Penetrating radar, internal structure, ice bed interface

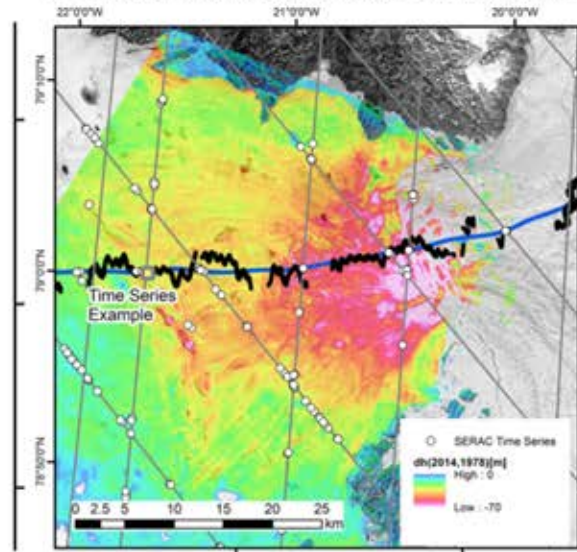


(Bell et al., 2014)

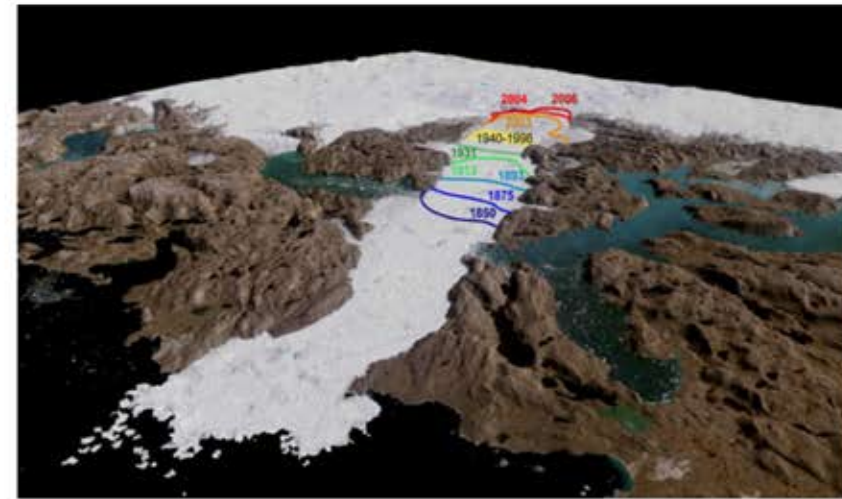
Upernivik Isstrøm, glacier 1; retreat of calving front in 2005, June 19, ASTER imagery



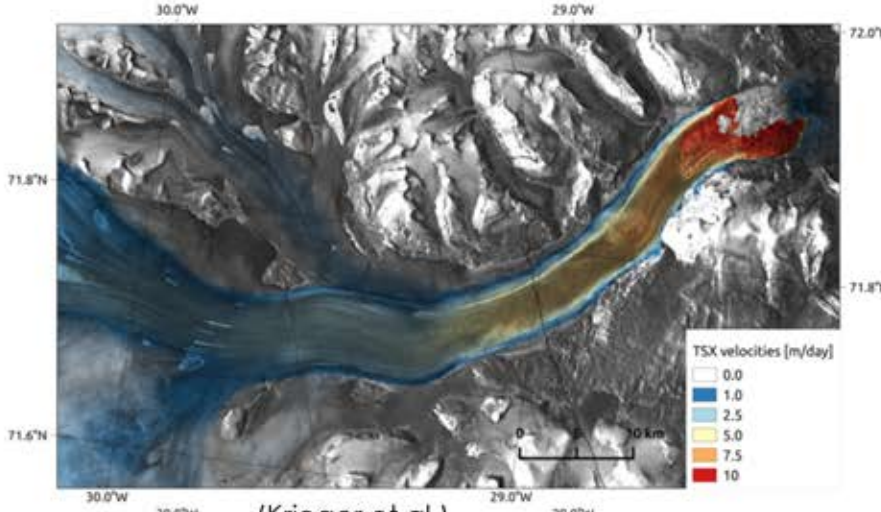
Zachariæ Isstrøm Ice thickness change from SPOT (2014) and aerial photo (1978) DEMs



Jakobshavn Isbræ retreat on draped Landsat mosaic

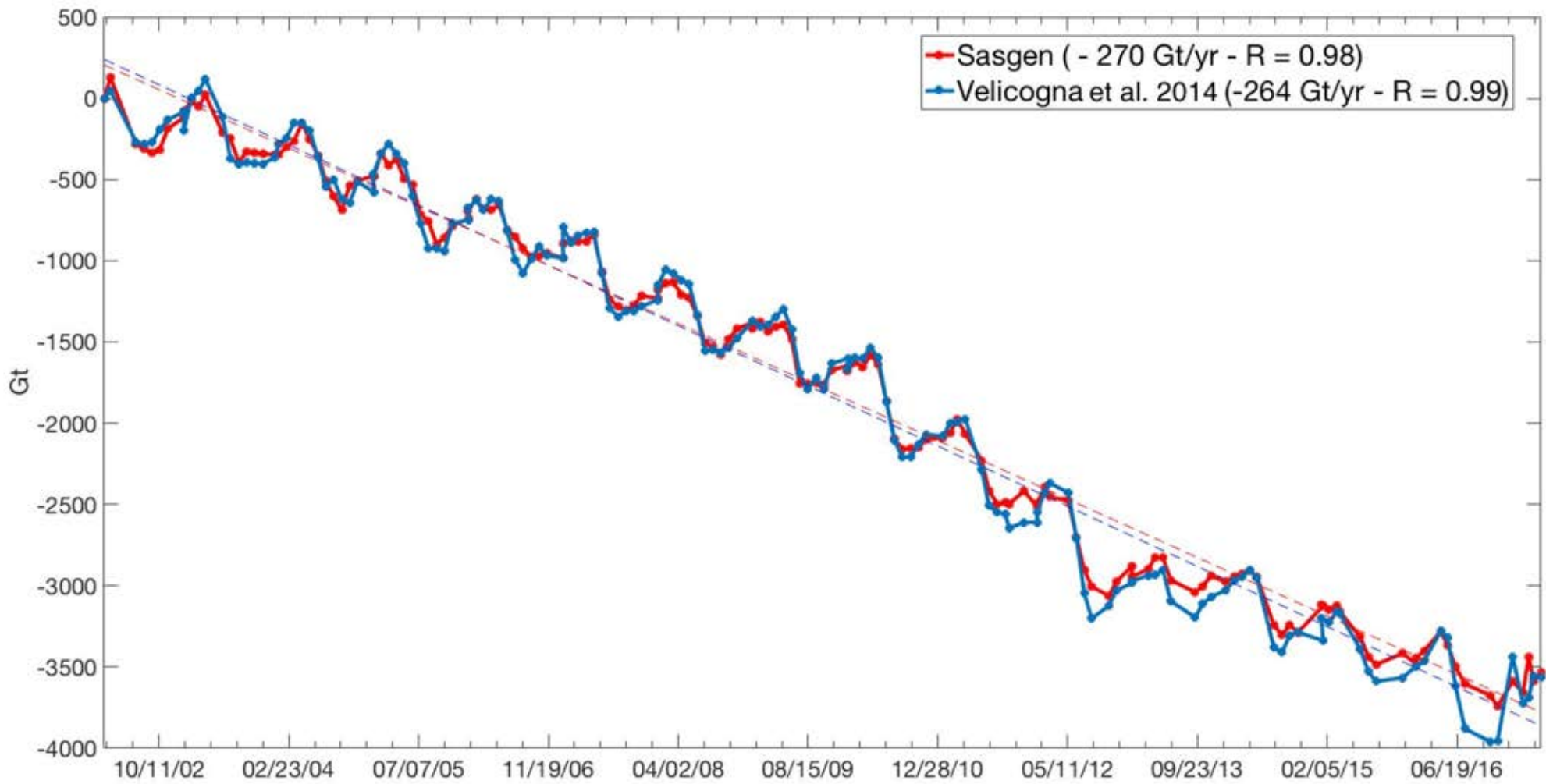


Velocity of Daugard-Jensen Glacier from TerraSAR-X

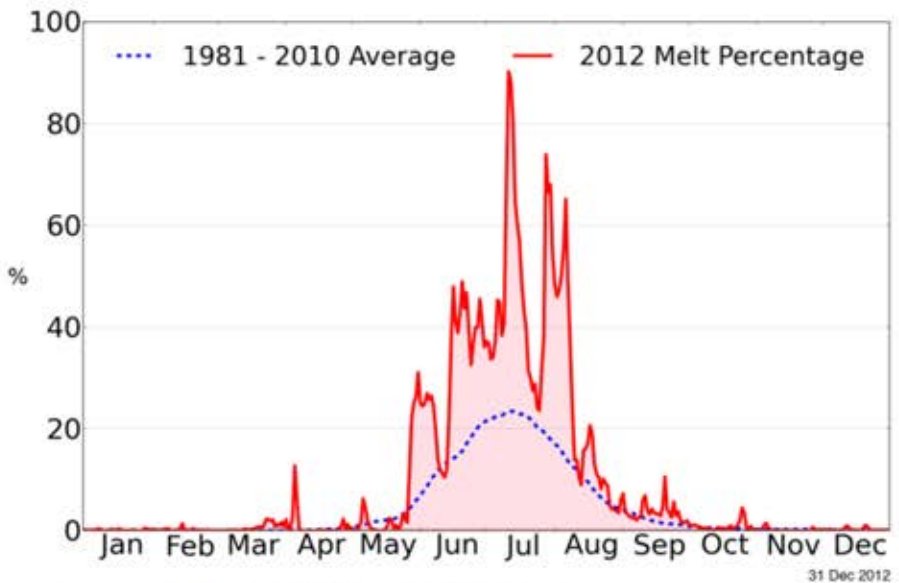


(Krieger et al.)

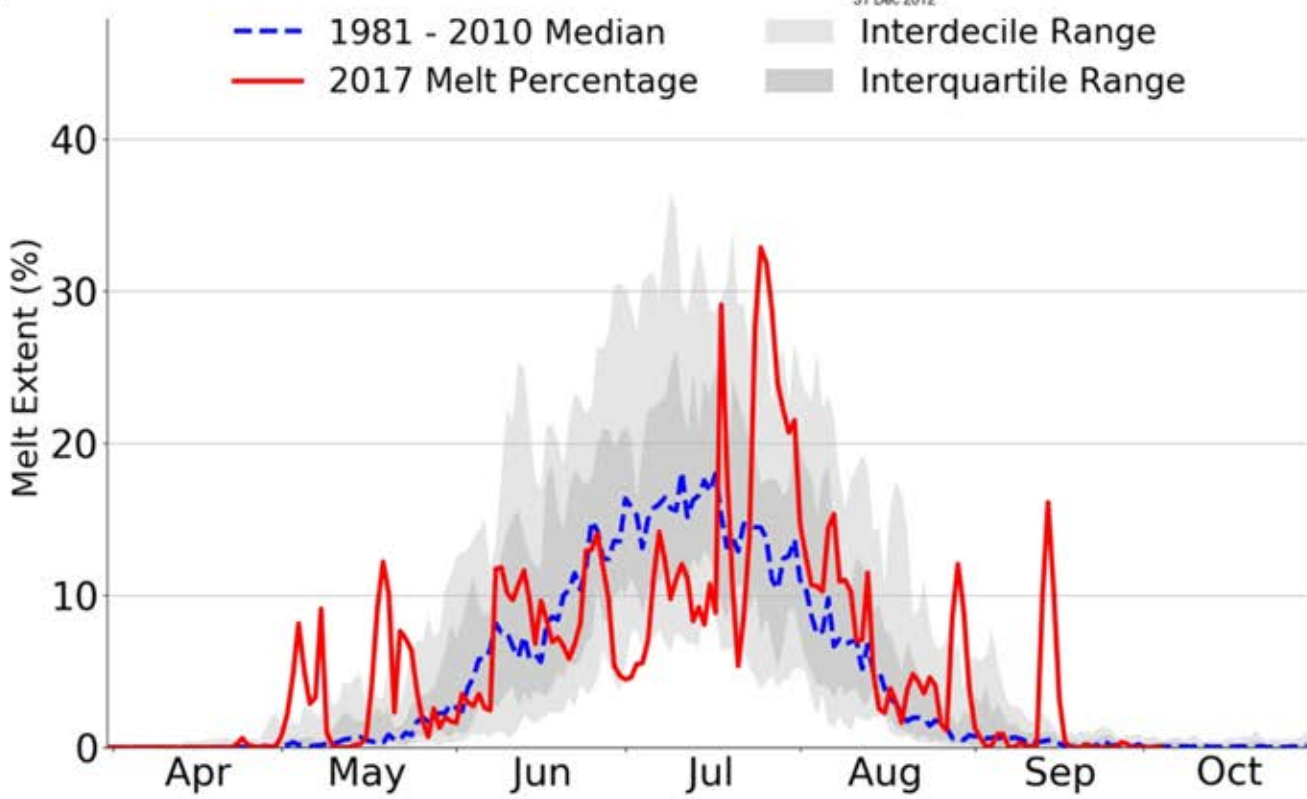
# Change in the total mass (in Gt) of the Greenland ice sheet between April 2002 and June 2017, estimated from GRACE measurements



## Greenland Melt Extent 2012



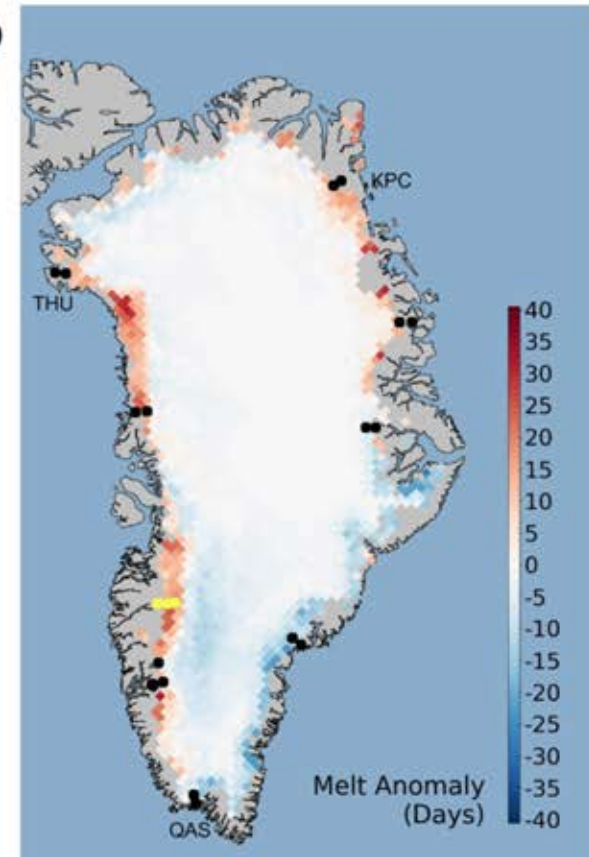
a



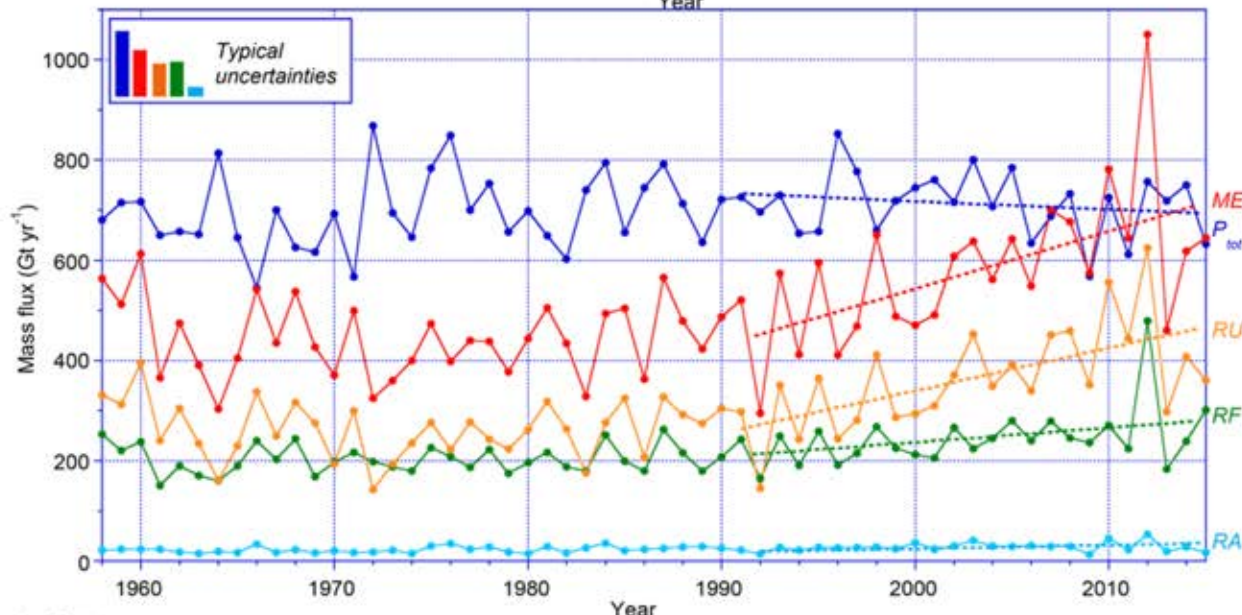
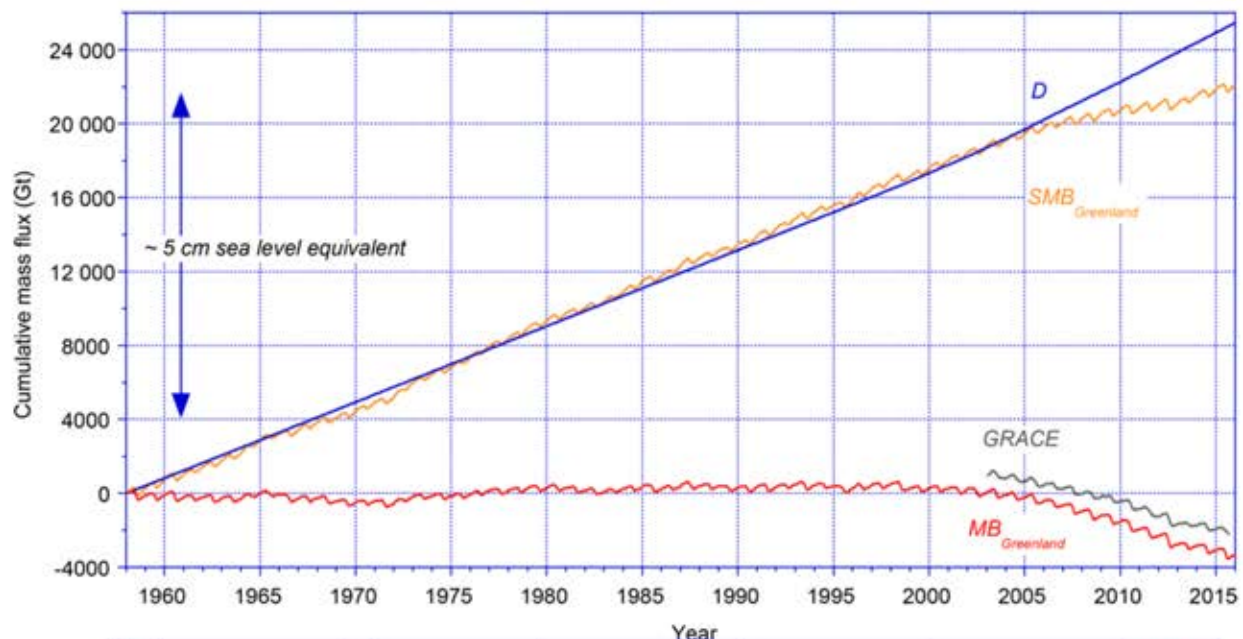
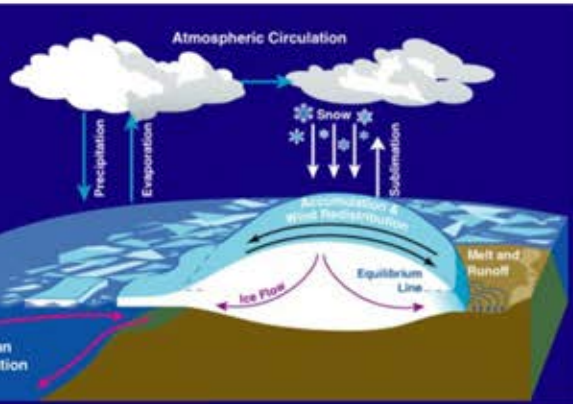
NSIDC / Thomas Mote, University of Georgia



b



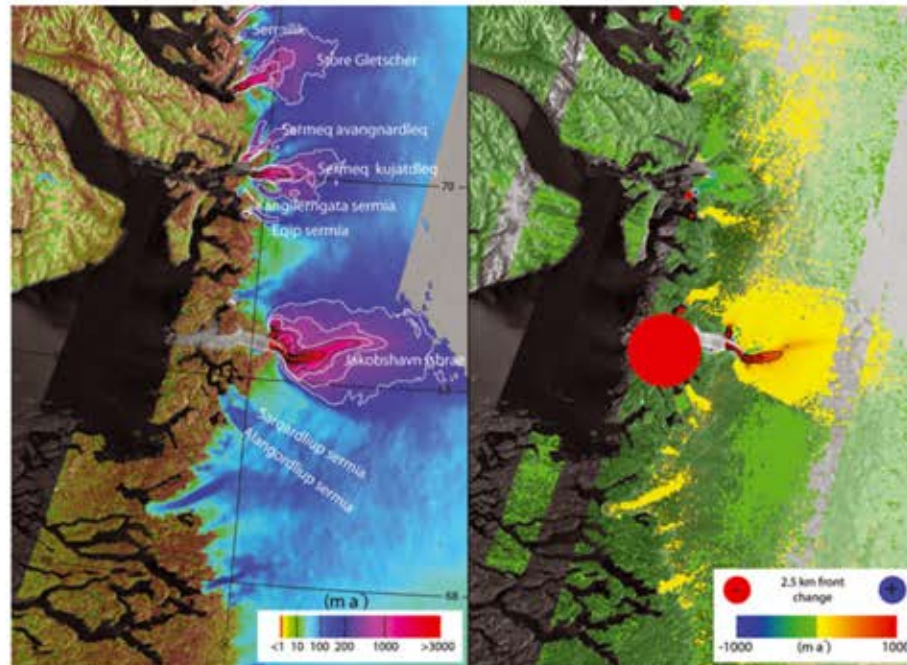
# Timing and main contributors to GrIS mass loss



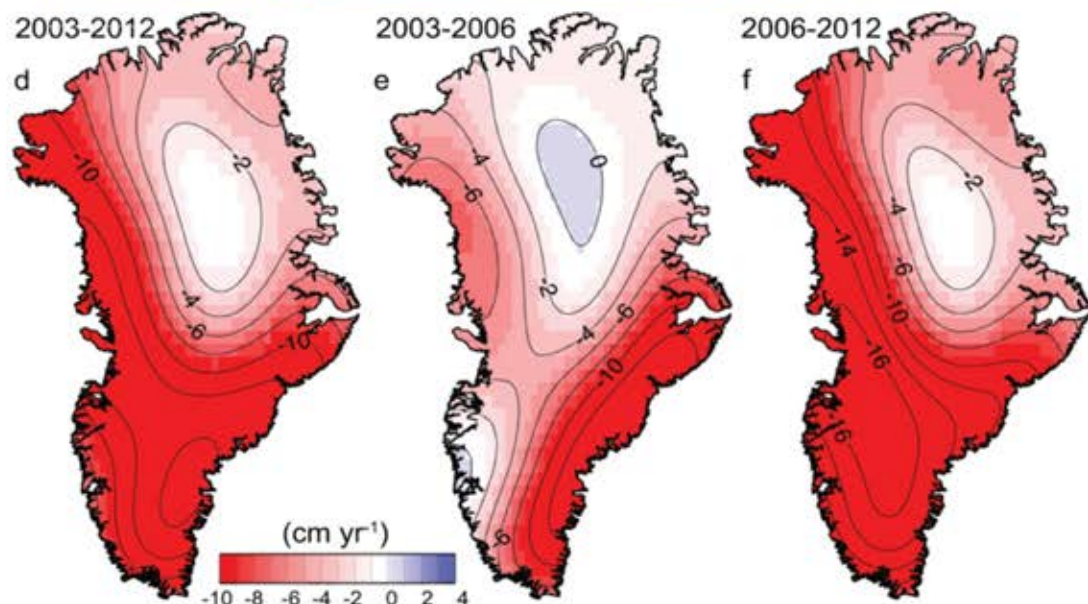
Total precipitation  
Melt  
Runoff  
Refreezing  
Rainfall

# Ice Sheet Velocity, Elevation and Mass Loss Patterns Change in Time

West Greenland flow speed for 2005/06 (left) and change in speed from 2000/01 to 2005/06 (right), from Joughin et al., 2010



Temporal evolution of ice loss determined from GRACE time-variable gravity, shown in cm of water per year (IPCC, AR5; Velicogna, 2009)



# Increasing the resolution of the GRACE record, mason solutions

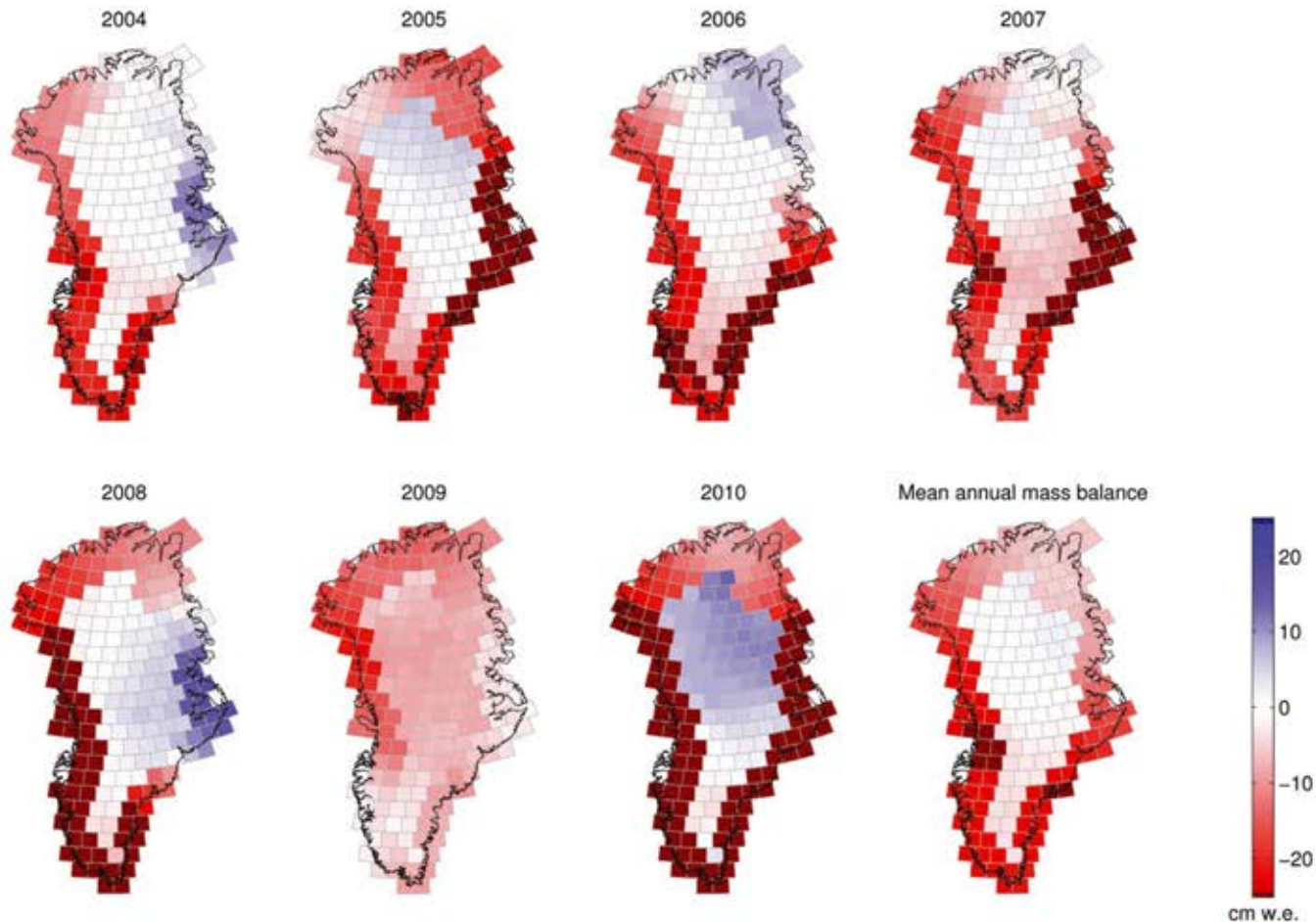
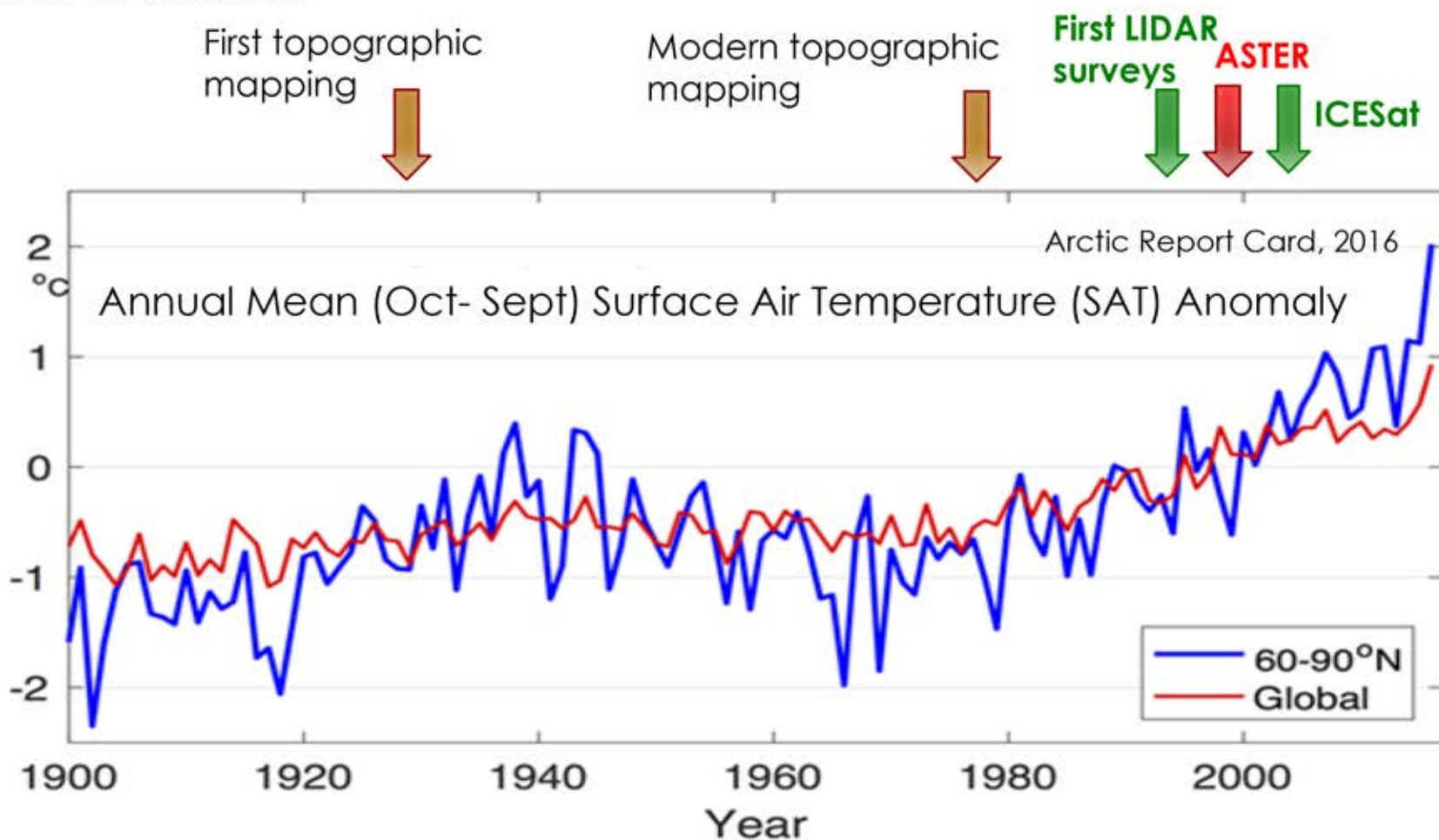


**Fig. 10.** The GIS annual mass balances and mean annual mass balance determined from the EEMD analysis of the v12 mascon solution. The timing of the seasons is determined by the mean EEMD extrema in Figure 8a, and the mass values are determined by the result of the EEMD method (summing the IMFs from the one preceding the 'annual' IMF to the final IMF) for each individual mascon time series at the time of the total GIS extrema.

Luthcke et al., 2014

Ice surface elevations provide a detailed record of past ice sheet extent, height and volume

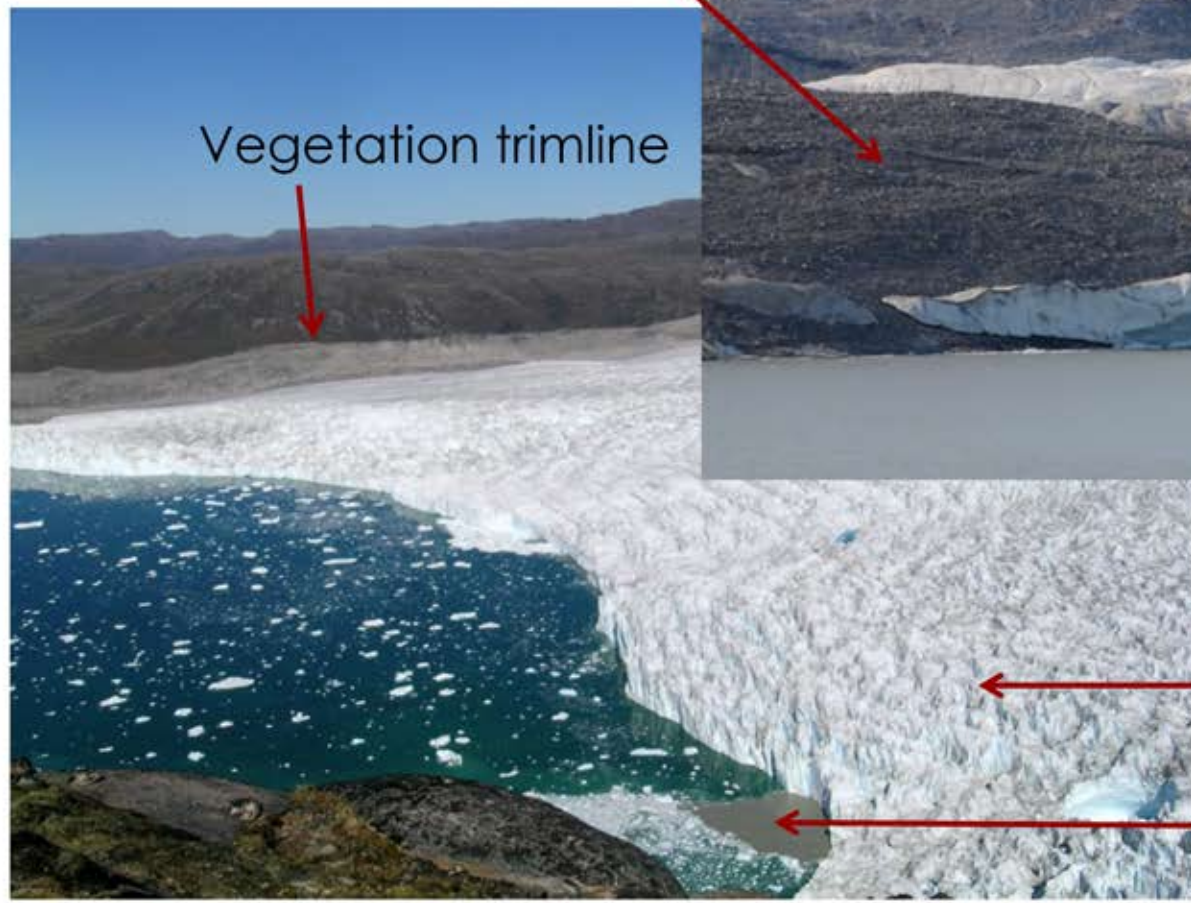


Aerial Photographs

Historical record and glacial geology

Laser altimetry

Free stereo satellite imagery, ASTER, WorldView

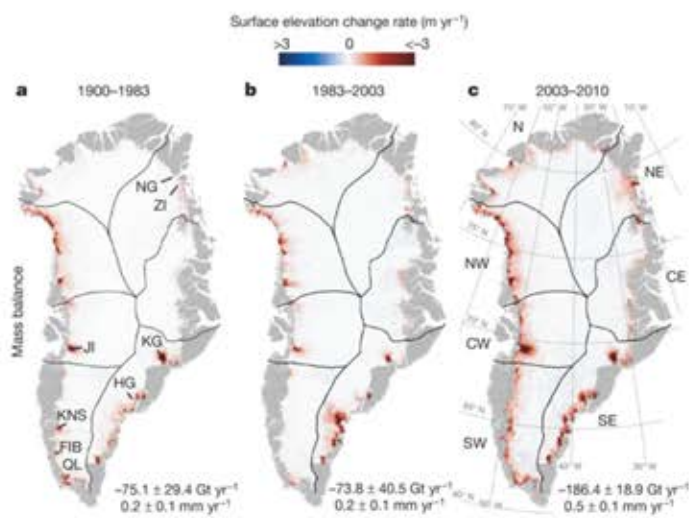


Ice sheet surface

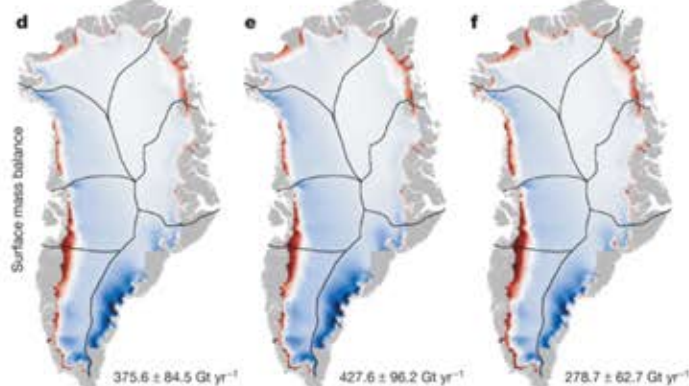
Sediment plume

# GrlS changes since the LIA show stable patterns for SMB and dynamics related surface elevation and mass changes

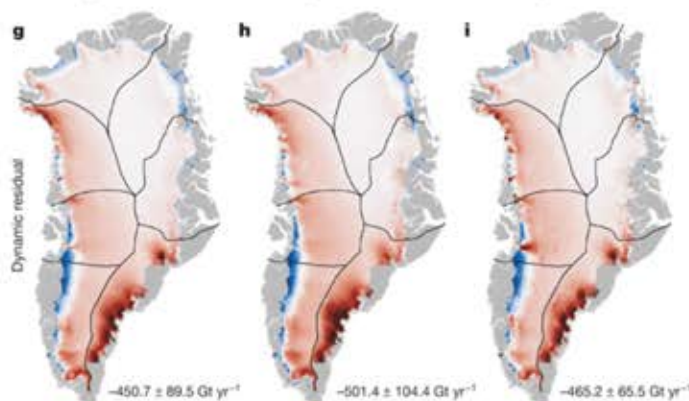
Total



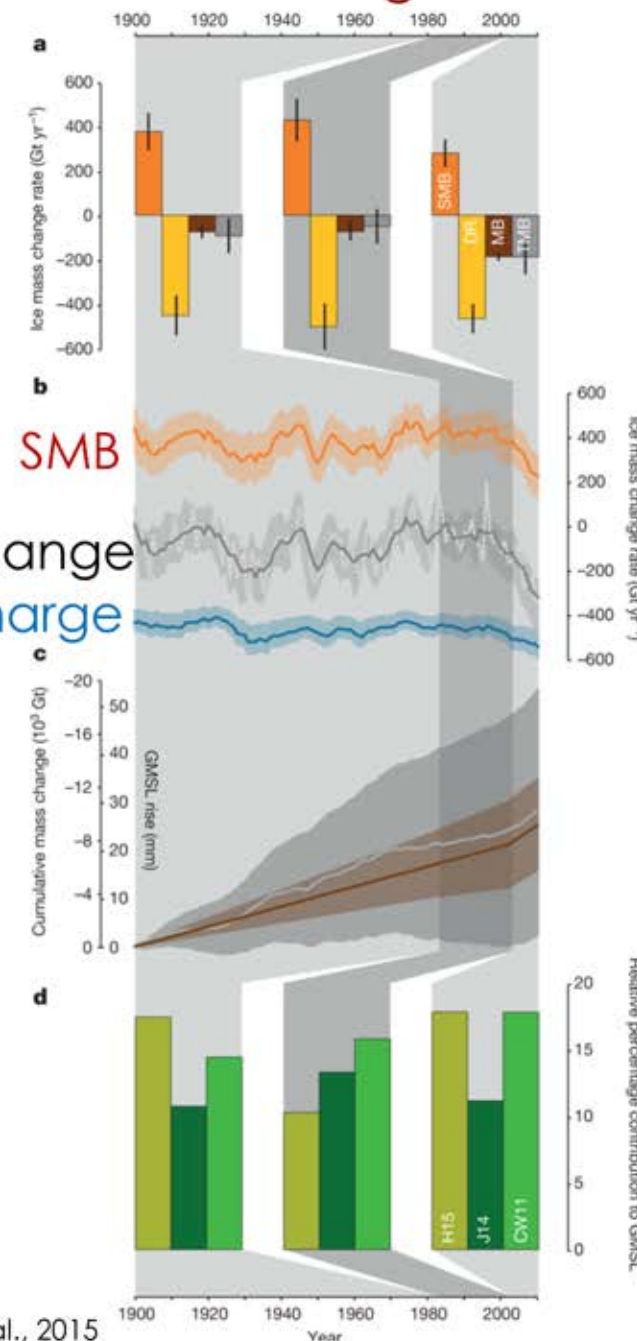
SMB



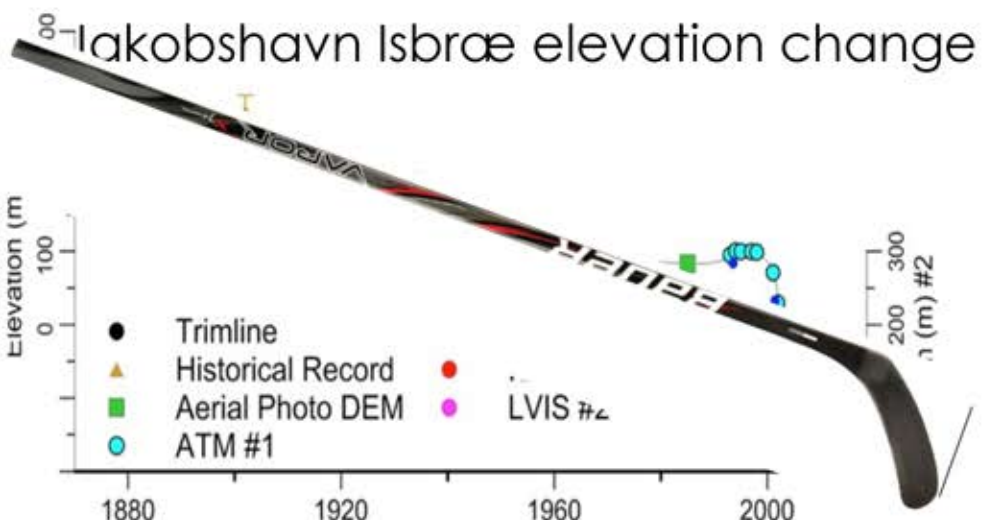
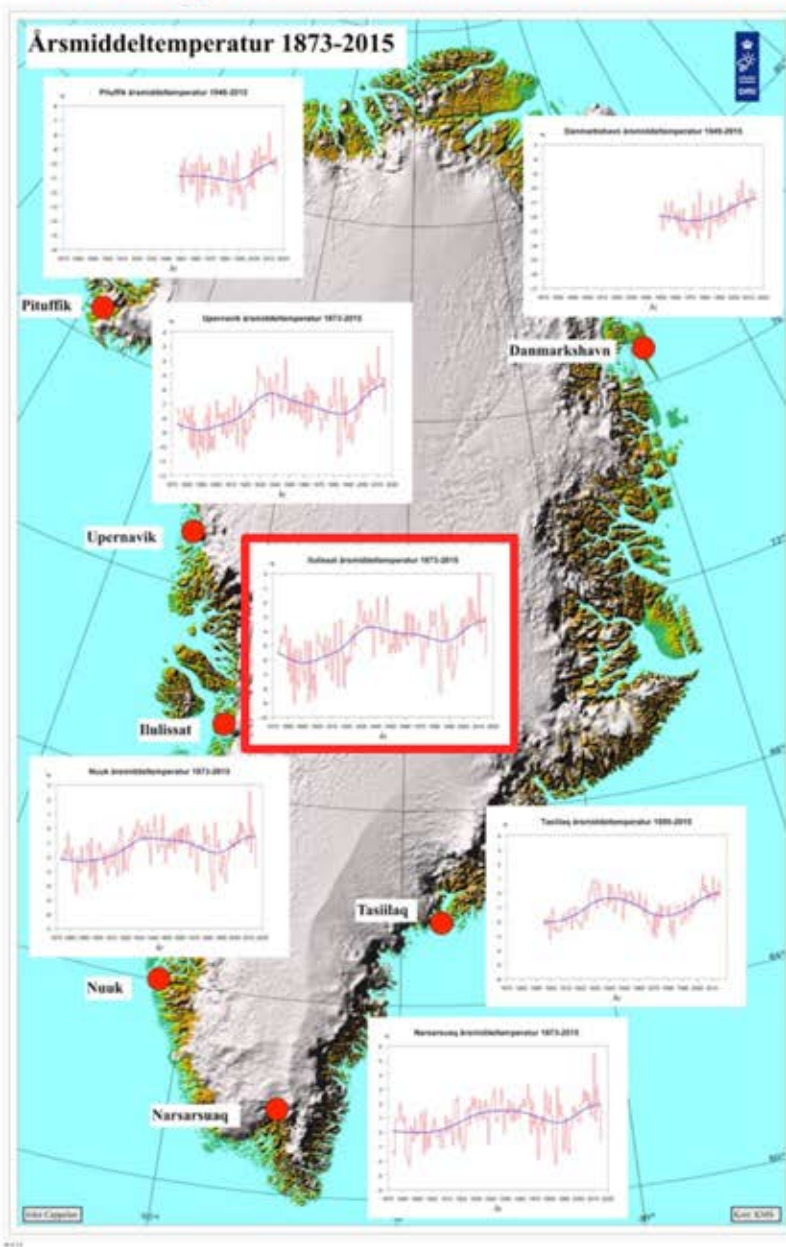
Dynamics



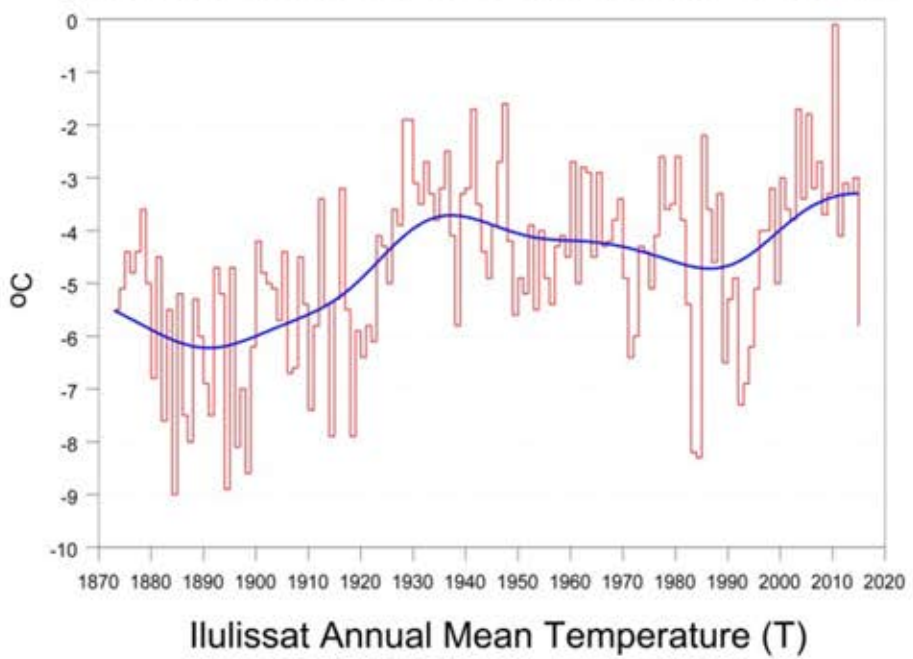
Kjeldsen et al., 2015



Long-term elevation change (proxy for mass balance) shows strong correlation with surface temperature, Jakobshavn Isbræ

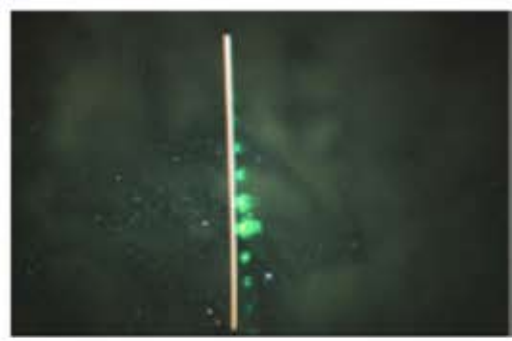
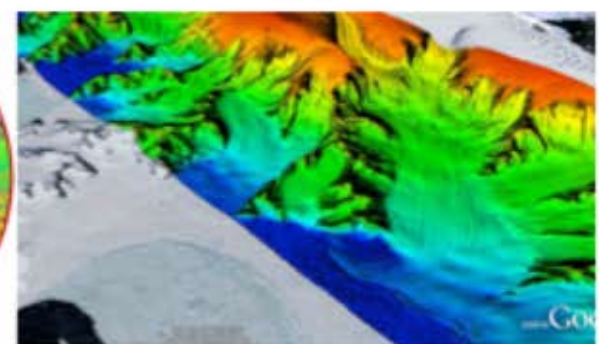
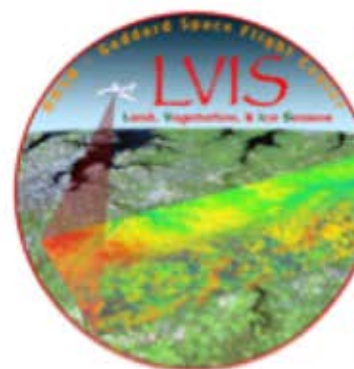


Ilulissat annual mean temperature

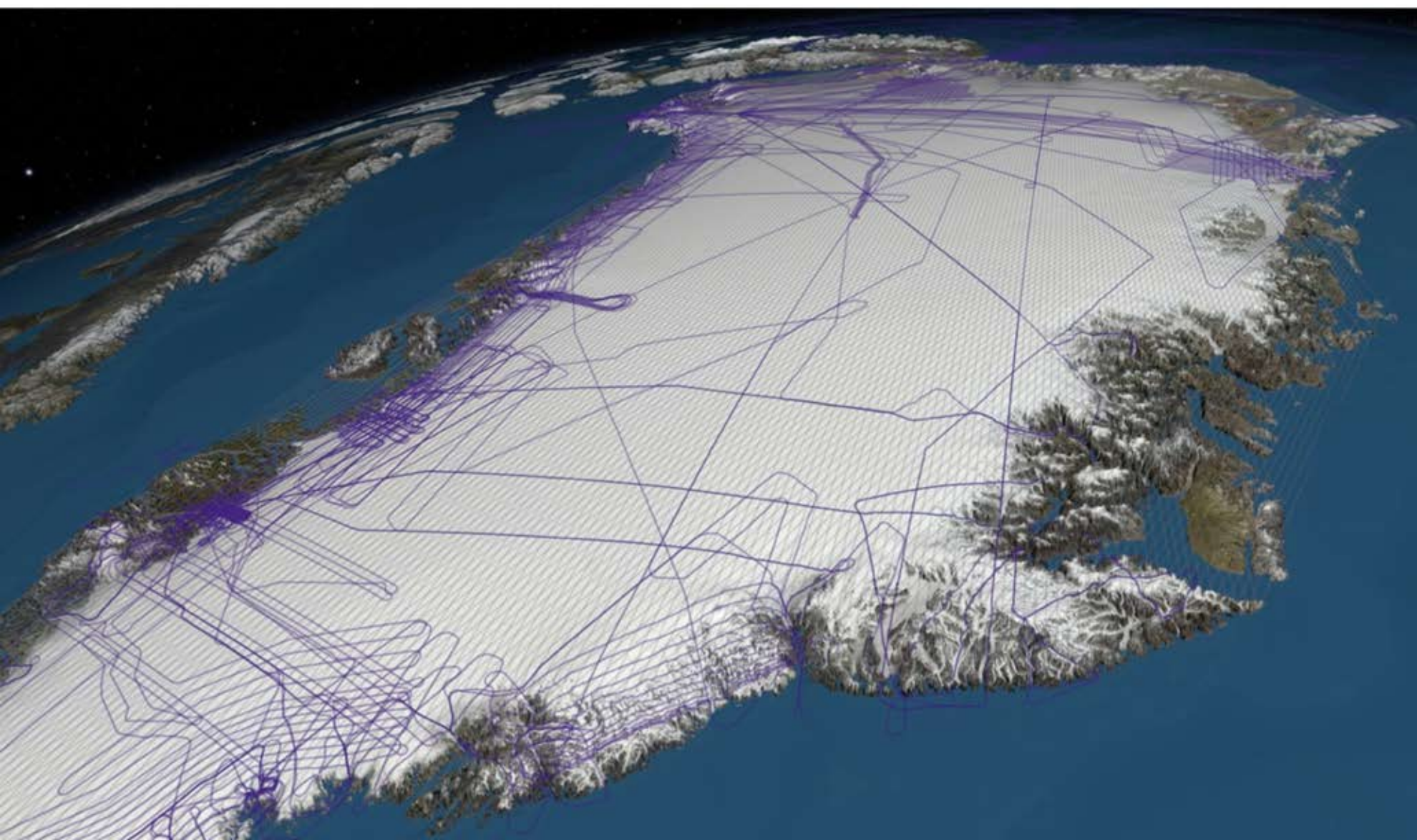


# The Altimetry Record Instruments

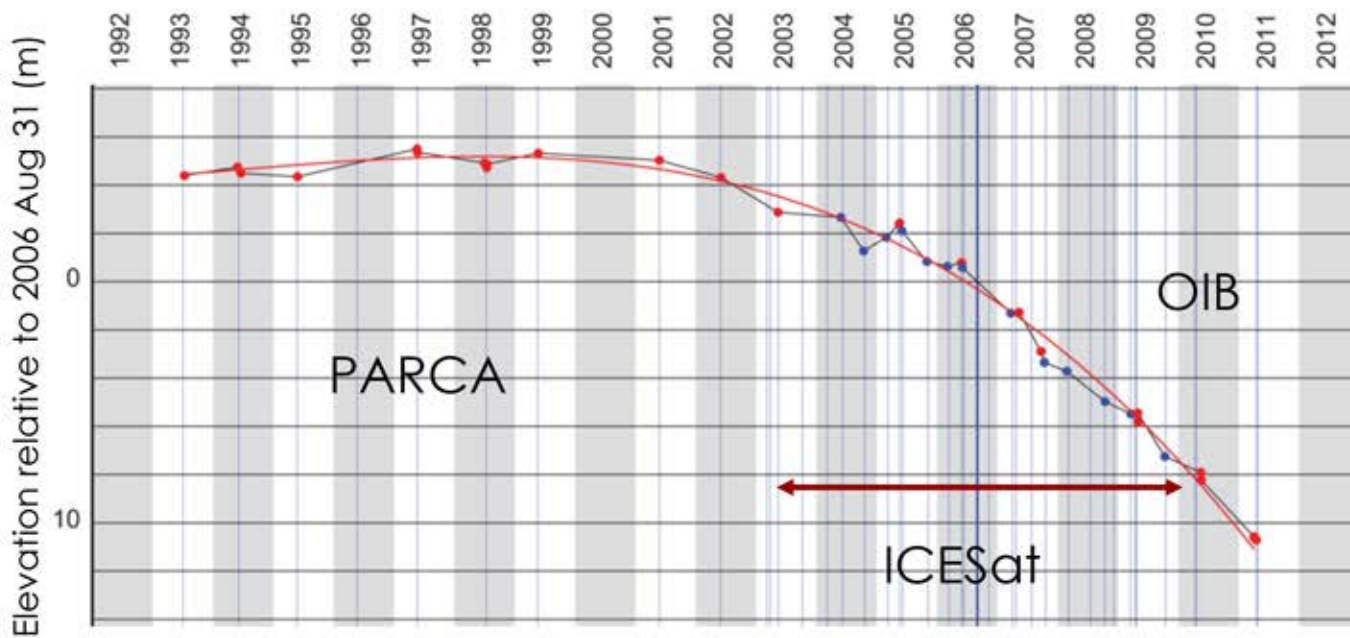
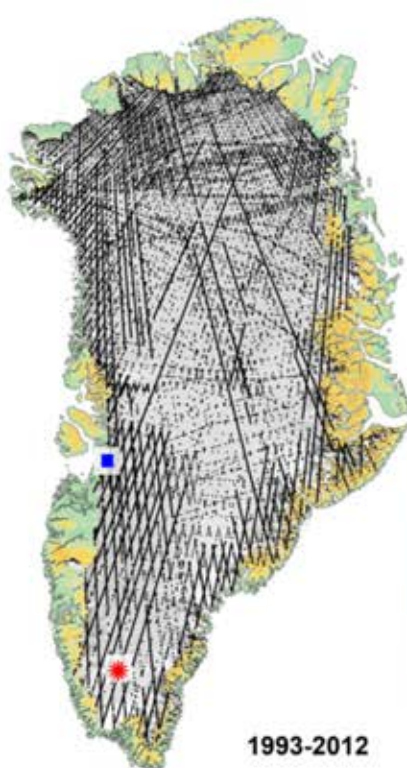
- Airborne Topographic Mapper (ATM)
  - 1993-present, airborne conical scanner with high repetition rate (kHz), small footprint size (1-3 m), covering 200-400 m wide swaths. ICESS data, 50-70 m platelet size are used
- Land, Vegetation and Ice Sensor (LVIS)
  - 2009-2013 (in Greenland), airborne line scanner with medium repetition rate and footprint size (20-25 m), covering 2 km wide swaths. Data set is reduced by applying plane fitting to obtain 50 m platelet size.
- Ice, Cloud and land Elevation Satellite (ICESat)
  - 2003-2009, satellite laser profiler with low repetition rate (40 Hz), large footprints (70-100 m) separated spaced by 170 m. All valid observations are used (criteria for energy and waveform fitting from Smith et al., 2009).



ICESat ground tracks (gray) and  
ATM/LVIS flight trajectories (purple)

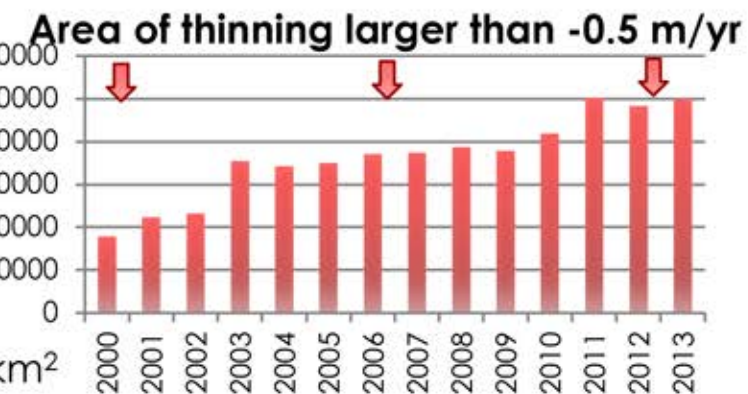


# The Altimetry Record: Methodology

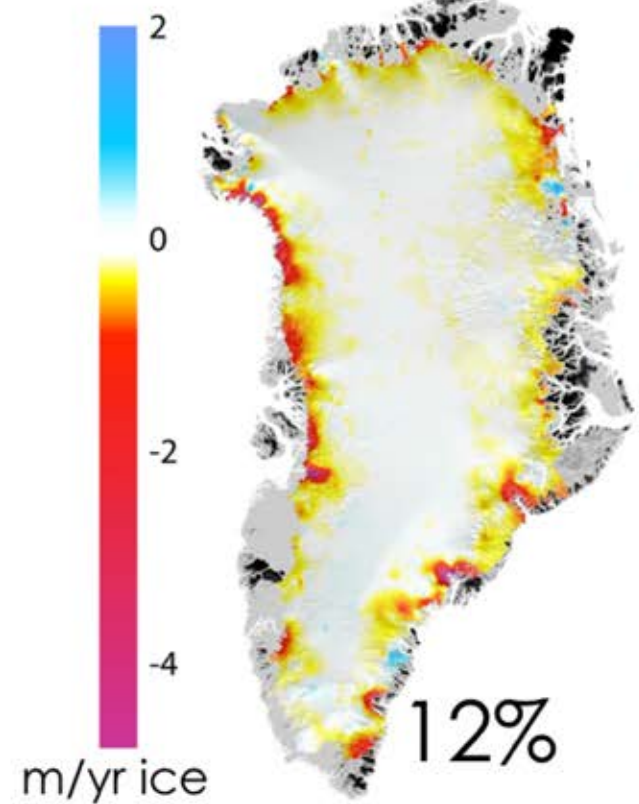


- Surface Elevation Reconstruction And Change detection (SERAC, Schenk and Csatho, 2012)
- Accurate and detailed ice surface change histories are reconstructed in more than 100,000 locations by combining all laser altimetry measurements on the Greenland Ice Sheet (Csatho et al., 2014, PNAS)

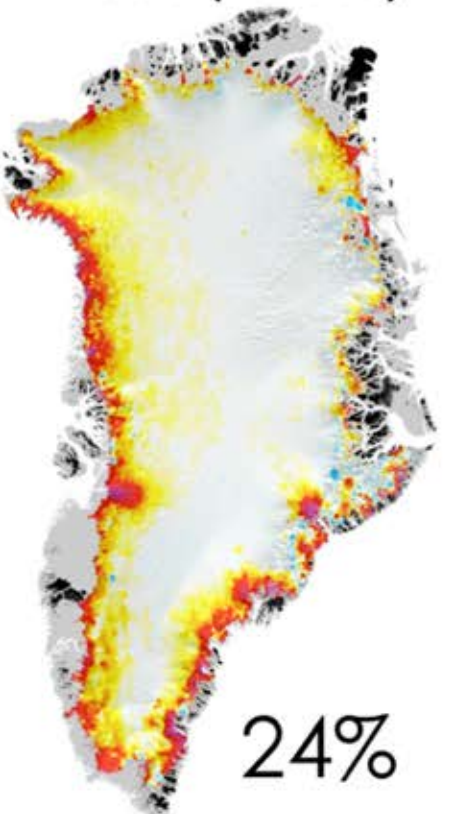
# OIB Measures the Increasing Extent of Thinning in Vulnerable Ice Sheet Marginal Region



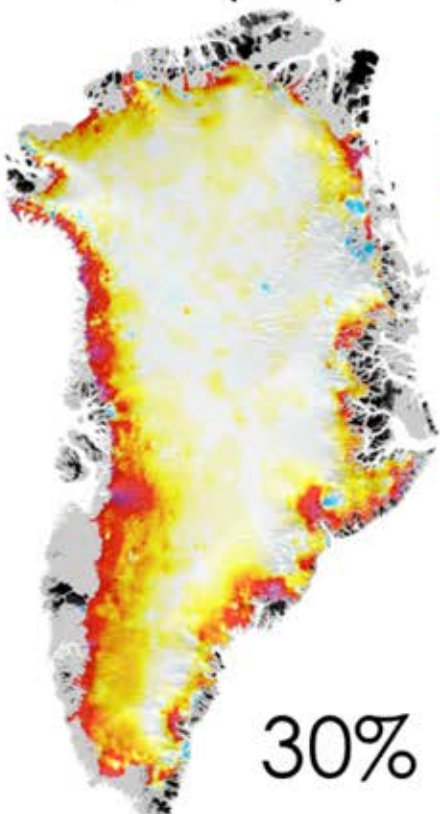
2000 (PARCA)



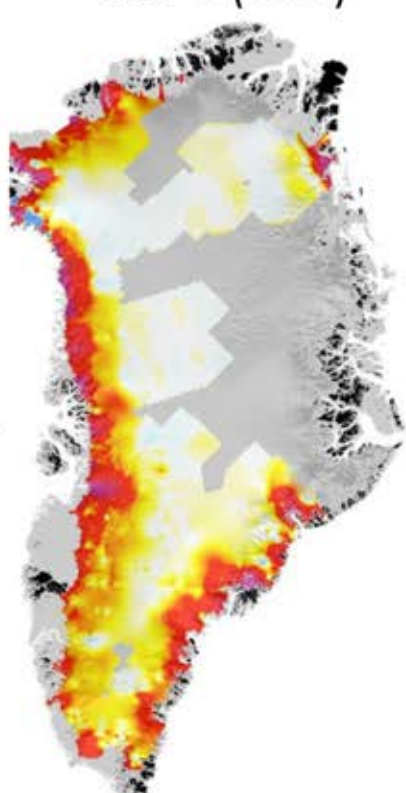
2006 (ICESat)



2012 (OIB)



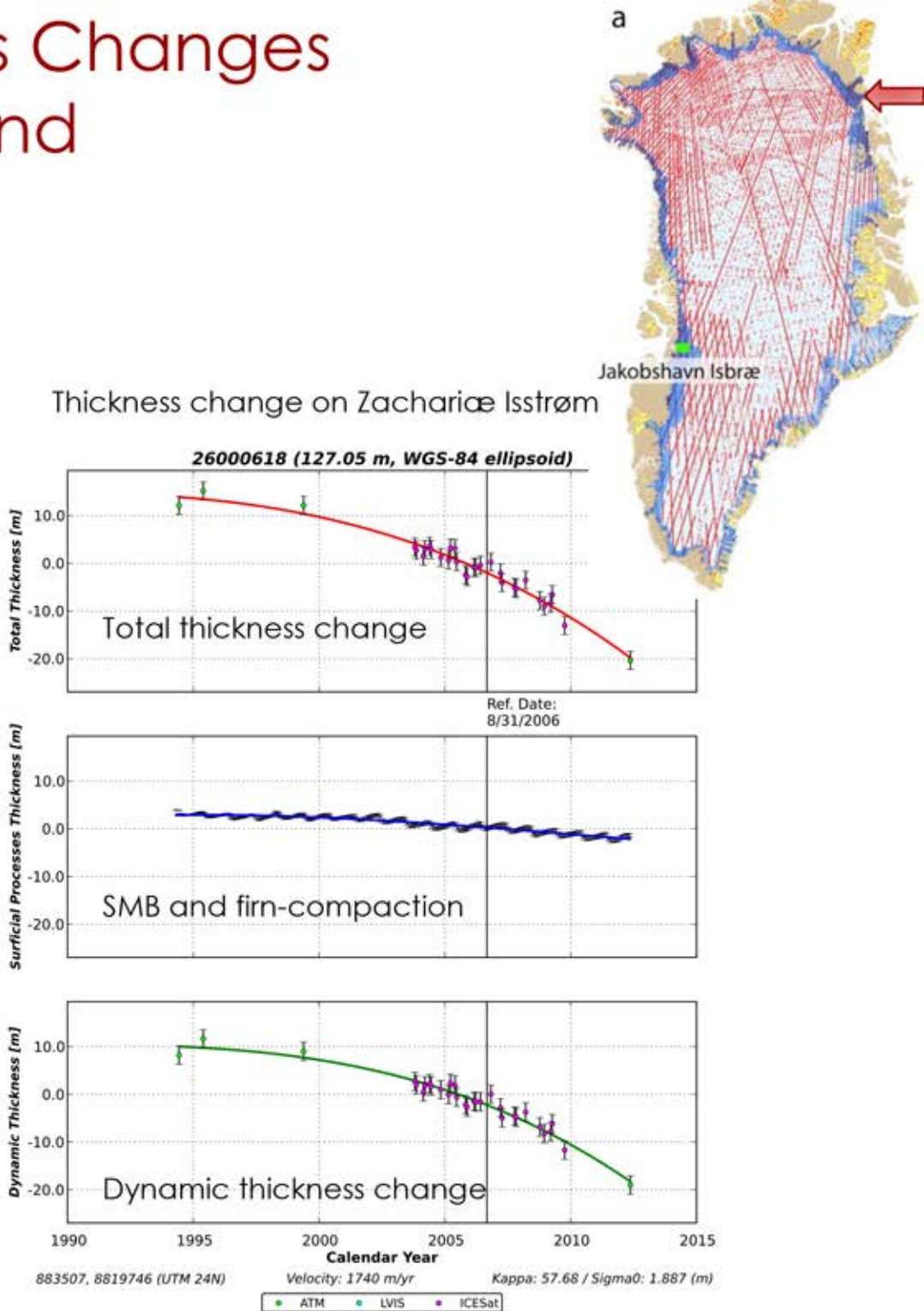
2014 (OIB)



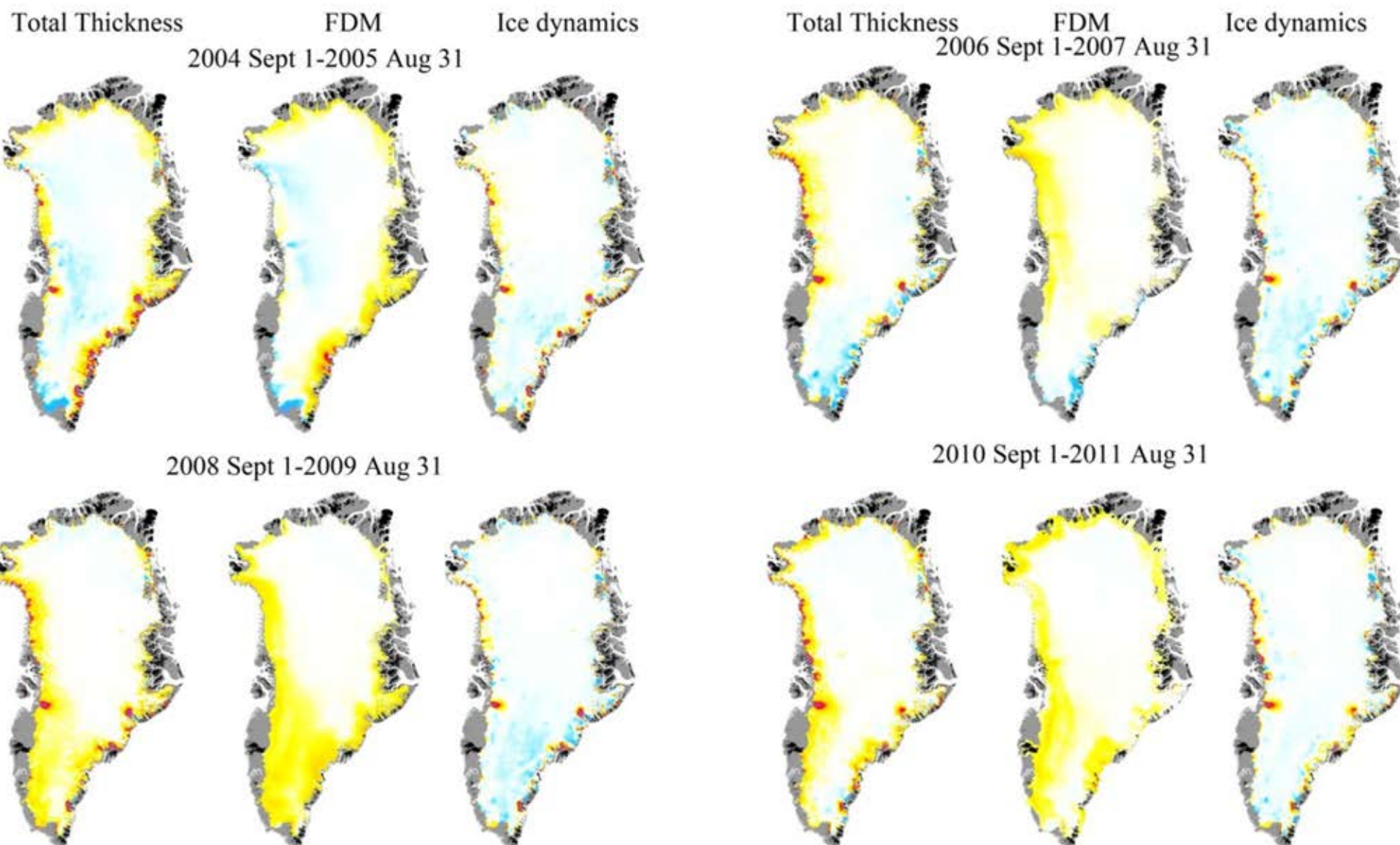
Percentage shows area with thinning rates of more than 0.5 m/yr, relative to total area below 2200 m elevation (790,000 km<sup>2</sup>)

# Partitioning Ice Thickness Changes into Surficial Processes and Ice Dynamics

- **Time series of ice thickness change**  
**(A)** from altimetry observations,  
corrected to remove Glacial Isostatic  
Adjustment
- **Firn densification (B)** from RACMO  
GR2.3 (FDM, Munneke et al., 2015)
- **Dynamic thickness change (C) =**  
thickness change reconstructed from  
altimetry observations (A) **minus**  
climate induced thickness changes on  
the surface (B)
- **Mass change** = dynamic thickness  
change (C)\*ice density + SMB  
anomaly
- **Annual change rates** are calculated  
from analytical curves fitted to times  
series

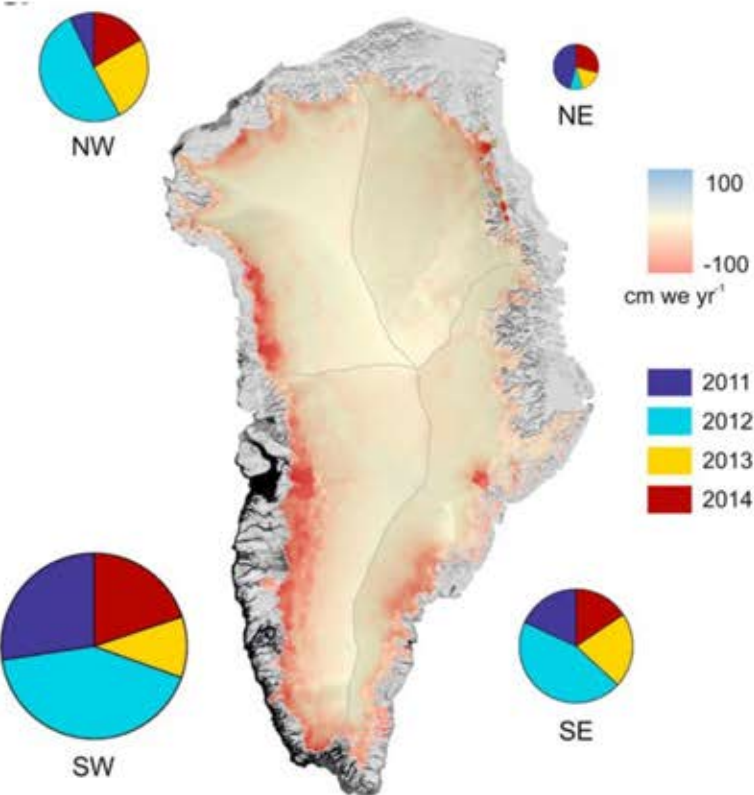


# A complicated puzzle: Interannual variation of ice thickness changes from laser altimetry, 2004-2010, partitioned into SMB (RACMO) and ice dynamics

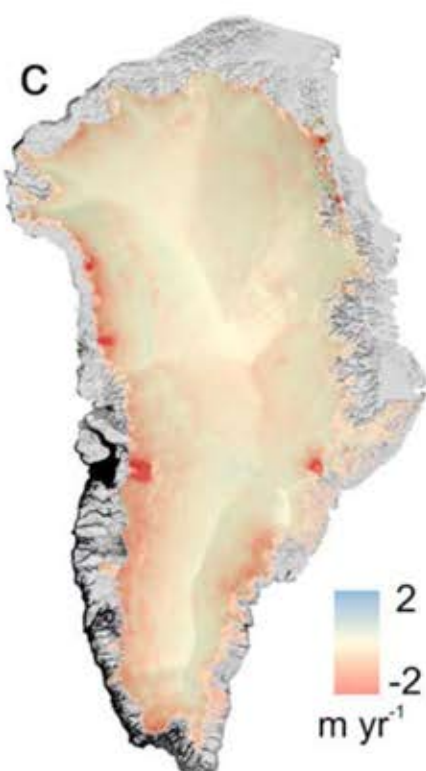


# Interannual variations in 2011-2014 from CryoSat-2 altimetry, McMillan et al., 2016

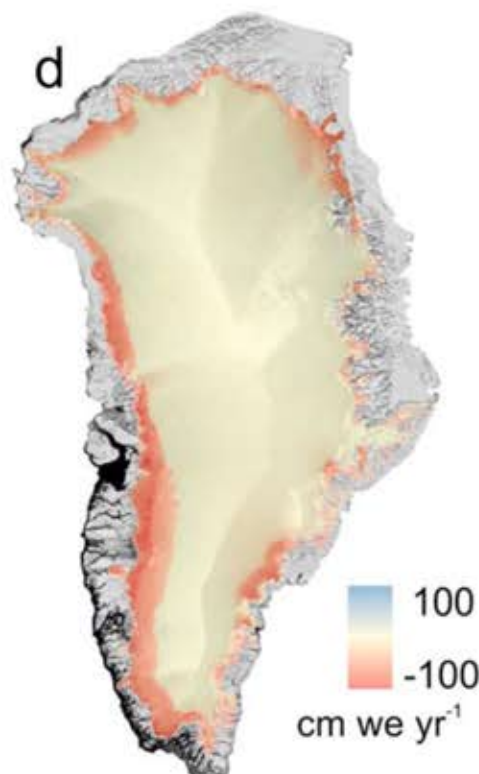
Mass change rate



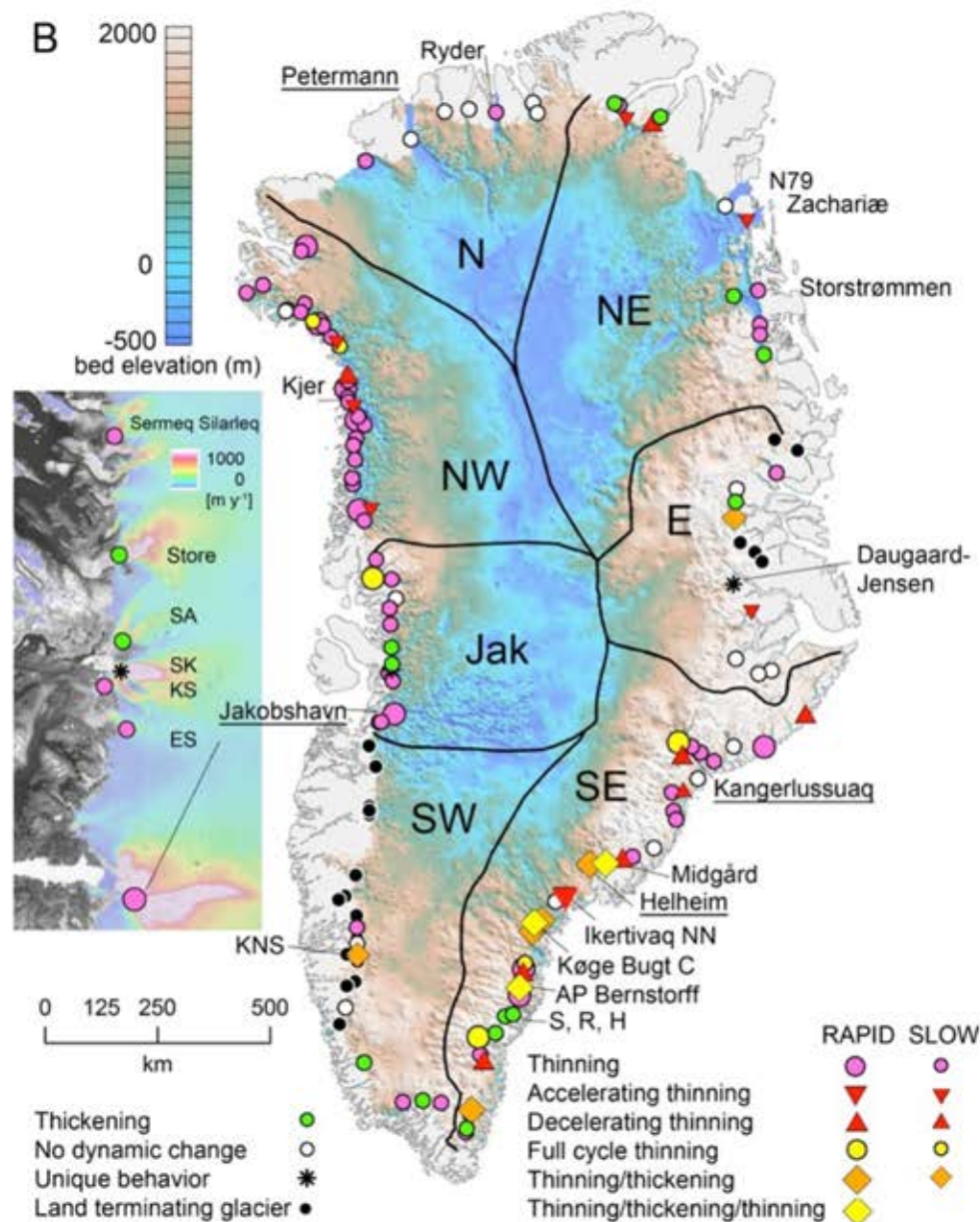
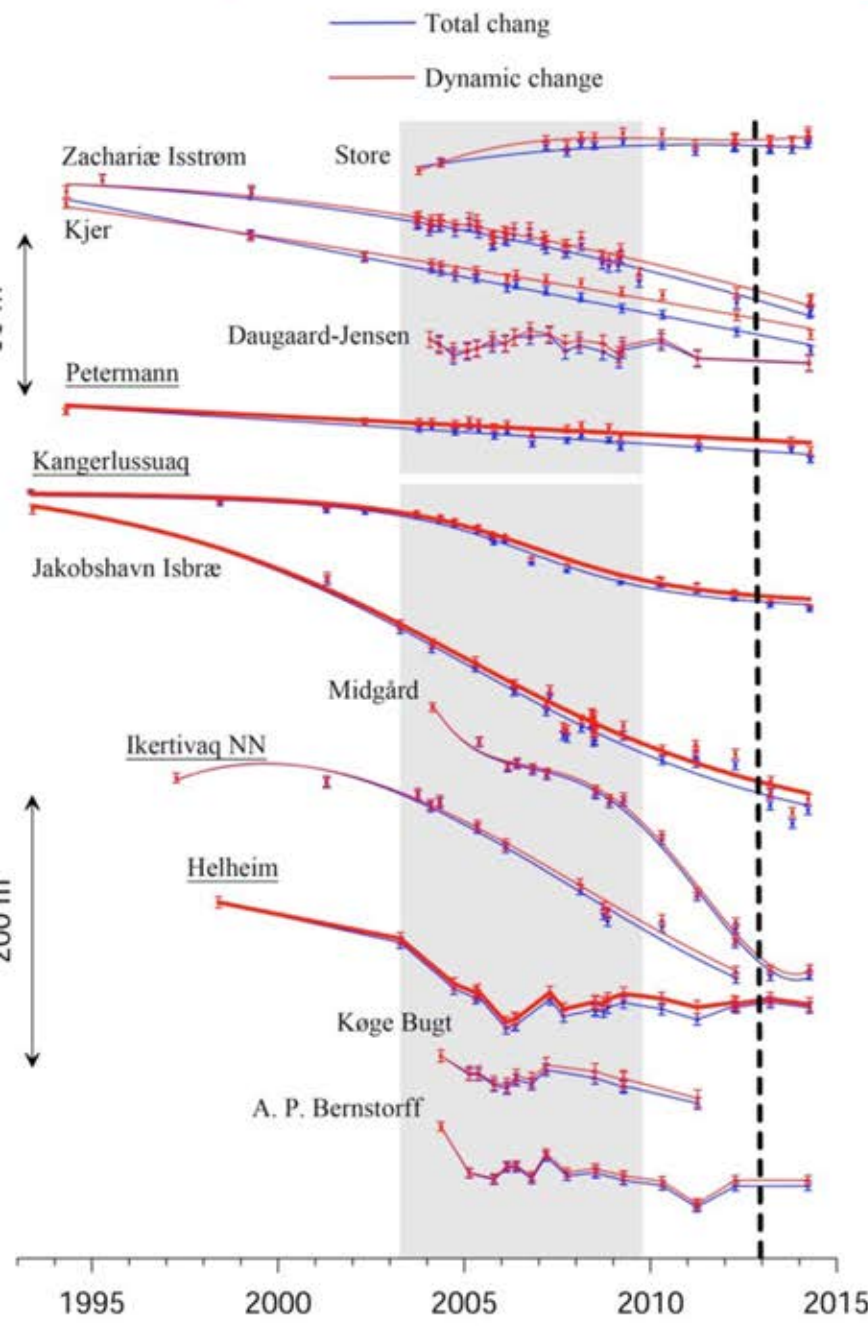
Total elevation  
change rate



SMB, RACMO2.3



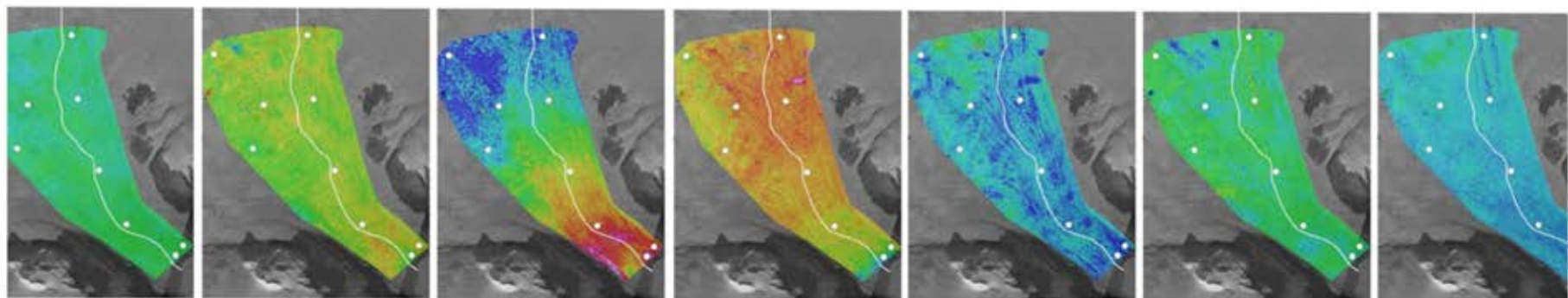
# Toward Process Understanding: Outlet Glacier Classification based on Dynamic Thickness Change Pattern (1993-2014)



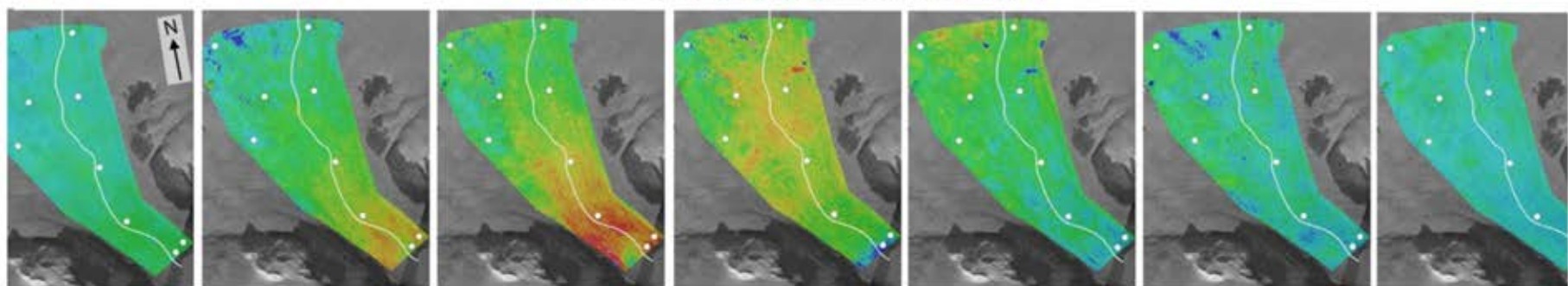
# Fusion of Altimetry with DEMs

- Correction of DEMs to remove systematic errors
- Spatiotemporal densification of surface elevation change histories
- Investigation of processes in 3D, extending study from repeat centerlines

Raw, uncorrected ASTER and SPOT DEMs



Corrected ASTER and SPOT DEMs



2001-03

2003-04

2004-05

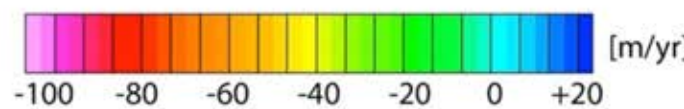
2005-06

2006-07

2007-08

2008-10

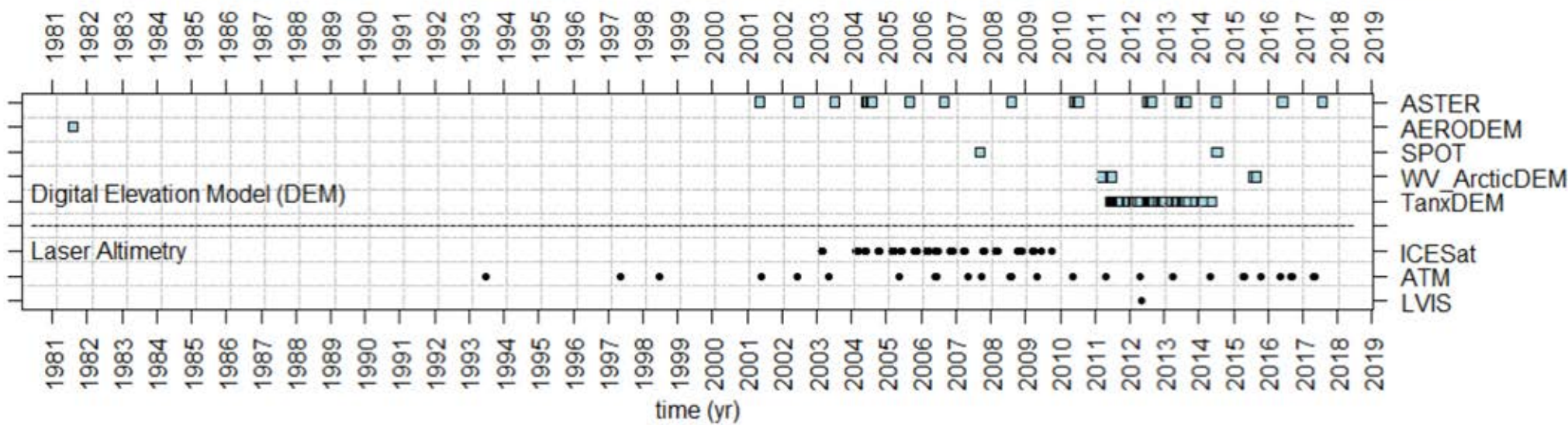
25 km



(Schenk et al., 2014)

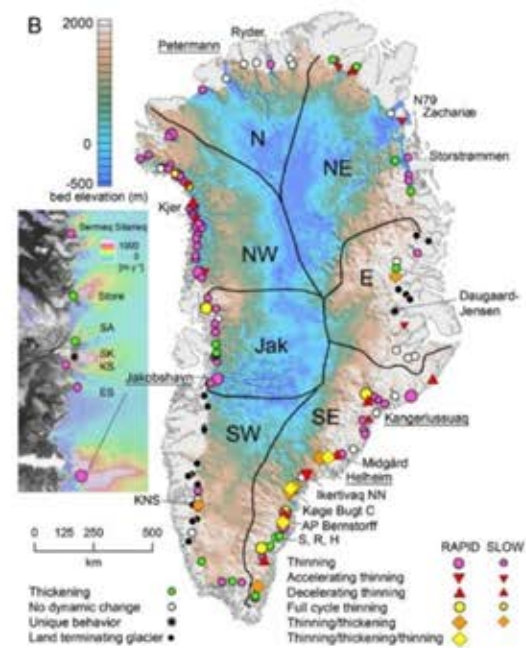
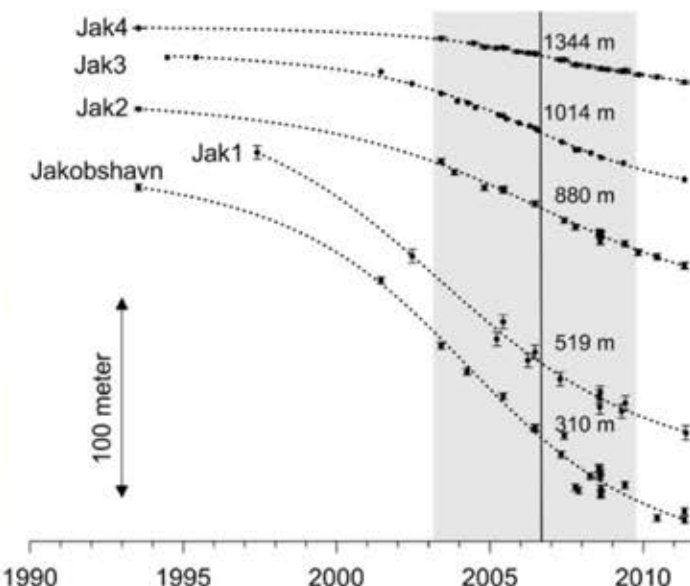
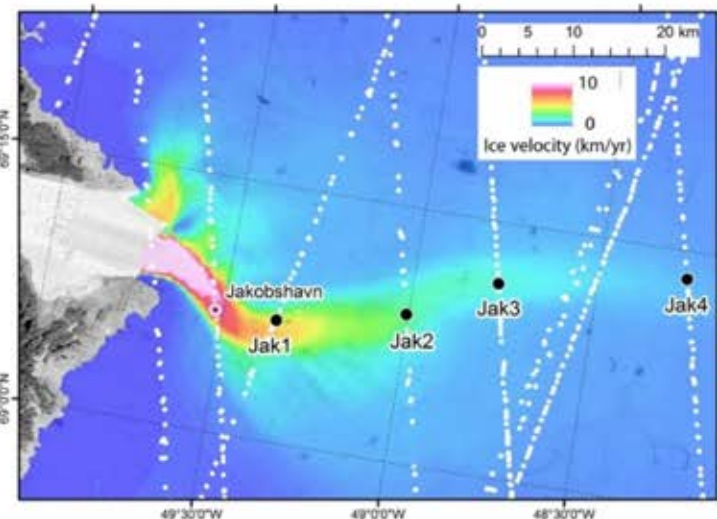
# Hydrological/sedimentary control on ice dynamics inferred at Helheim Glacier from robust elevation record

Robert et al., in prep.

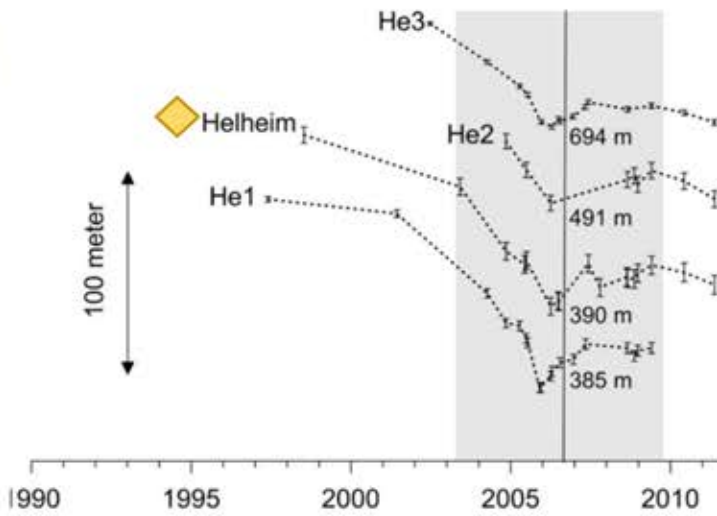
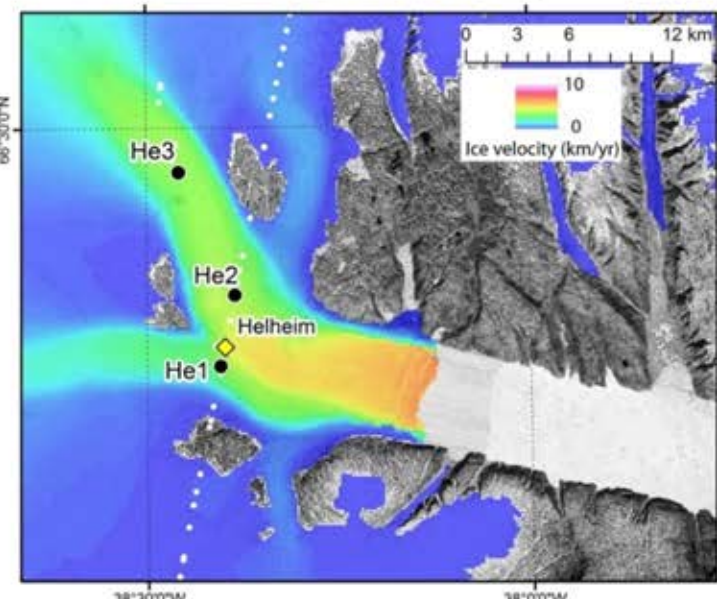


# Motivation: Normal glacier behavior vs. complex

- Jakobshavn Isbrae: Thinning is delayed and decreases in magnitude inland

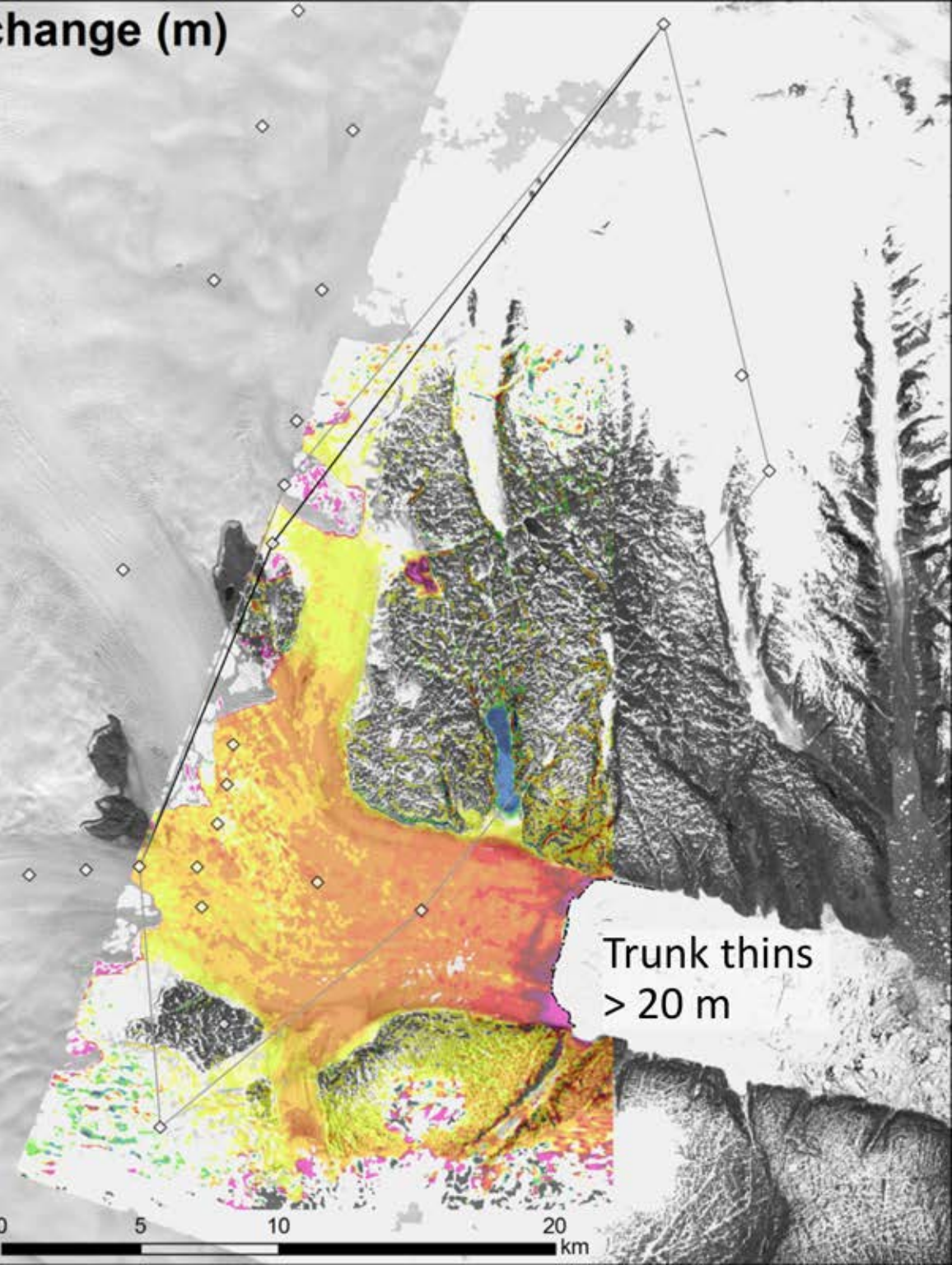
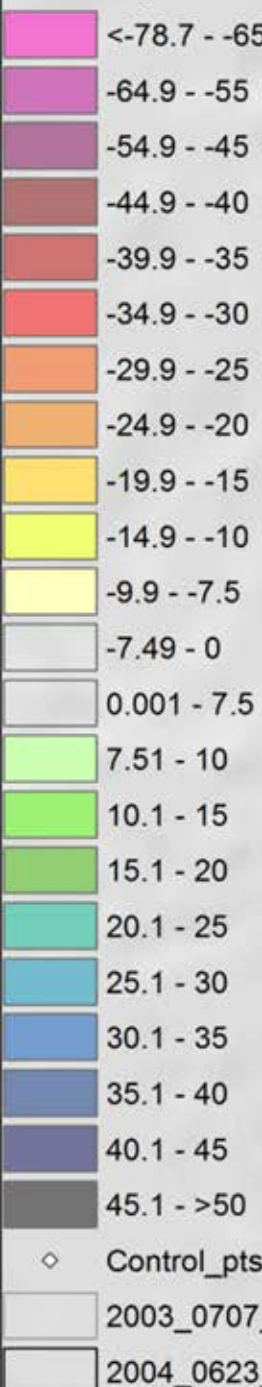


- Helheim Glacier: Irregular thickness variations = a separate, high-frequency process

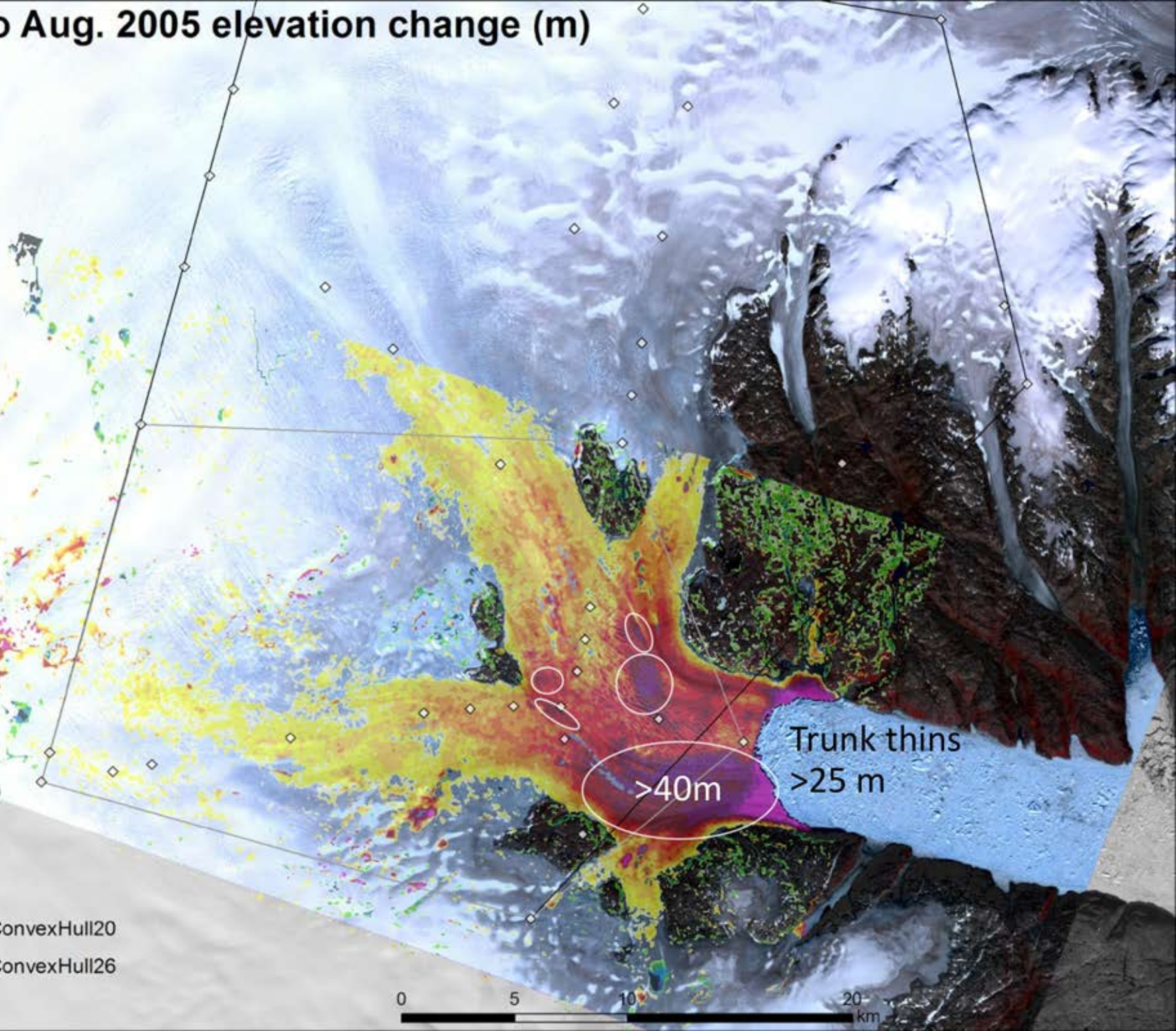
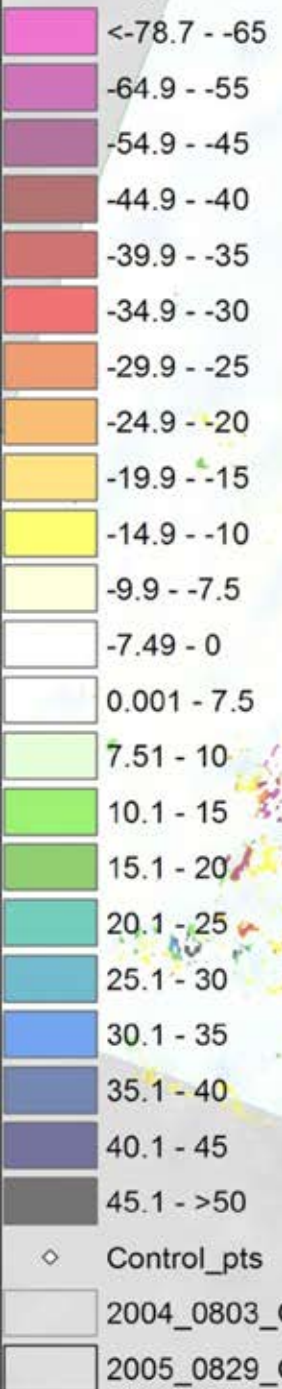


- Helheim Glacier behaves similarly even 20+ km from terminus

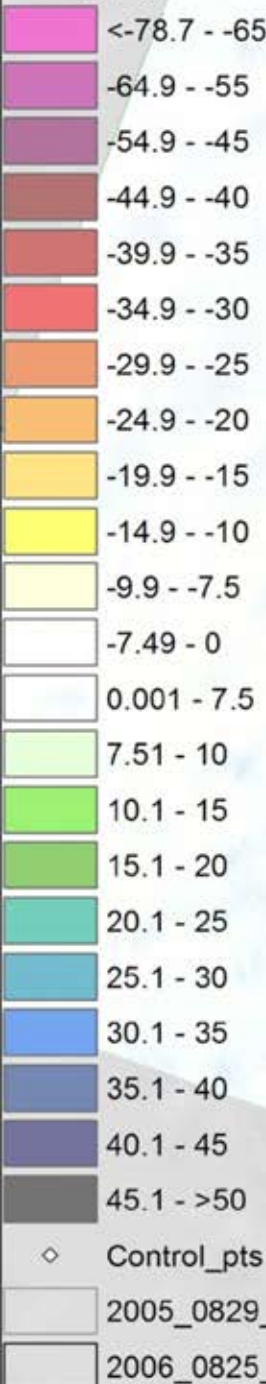
# Jul. 2003 to Jun. 2004 elevation change (m)



# Jul. 2004 to Aug. 2005 elevation change (m)



# Aug. 2005 to Aug. 2006 elevation change (m)



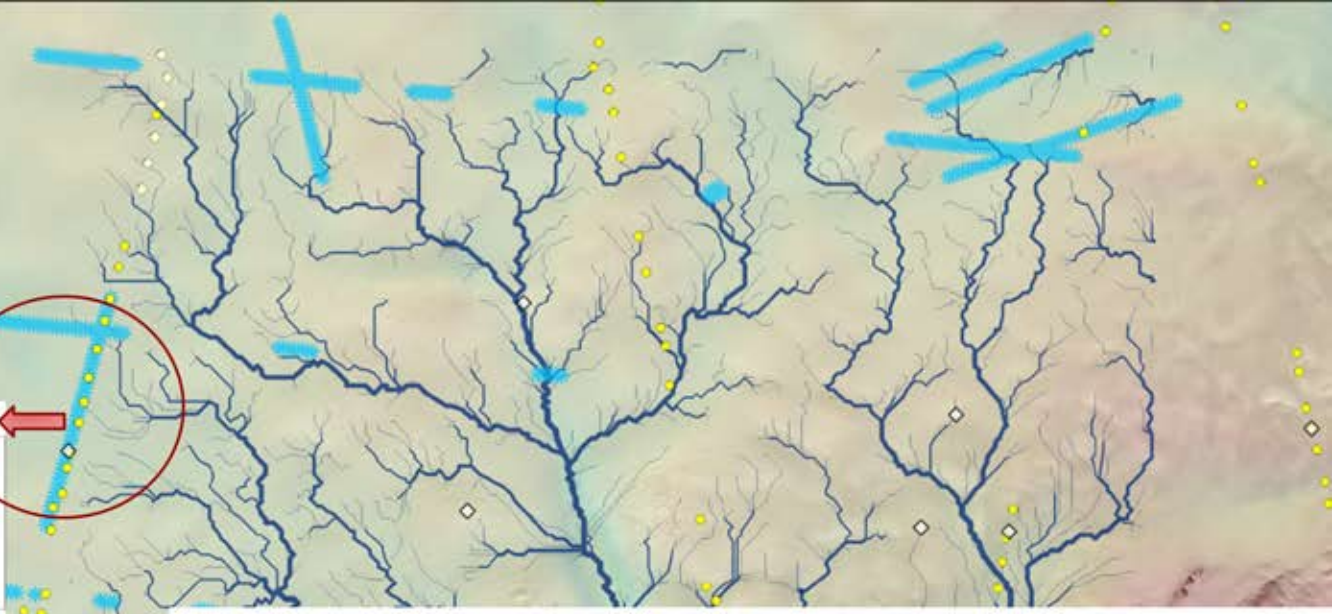
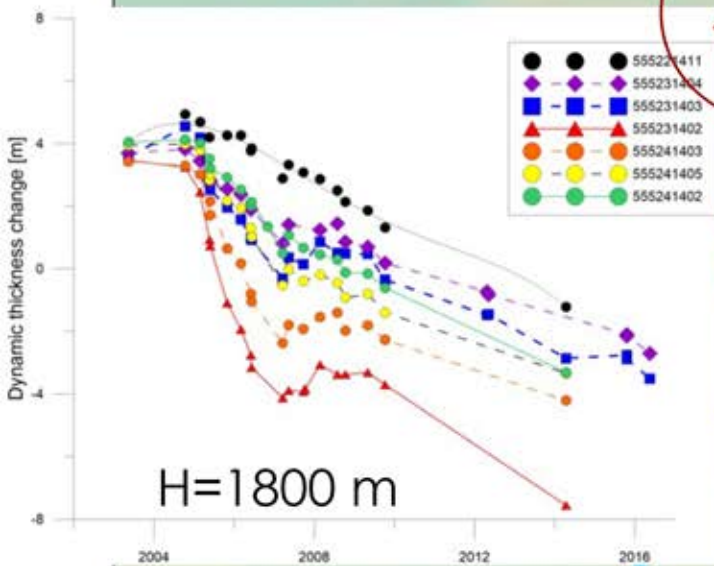
Patches on trunk  
*thicken 10-20 m*

Patches on Main  
& SW tributaries  
thin >11 m

CLOUDS

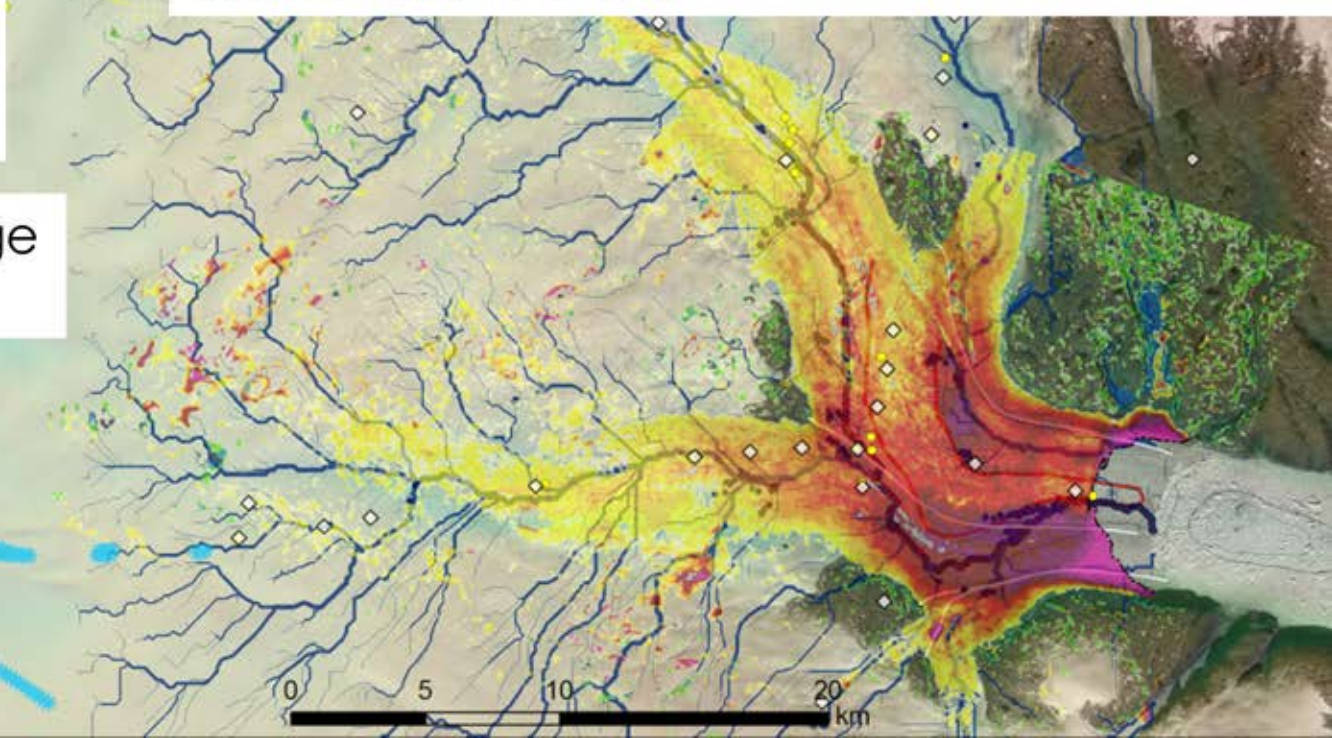
0 5 10 20 km

- Control\_pts
- Aquifer\_picks\_Miege et al., 2016
- Bedrock\_ridge
- Medial moraines
- Lakes
- Water-filled crevasses
- SERAC\_Dynamic\_curves\_2018



2004 July 2005 August elevation change attributed to enhanced deformation water saturated sediments

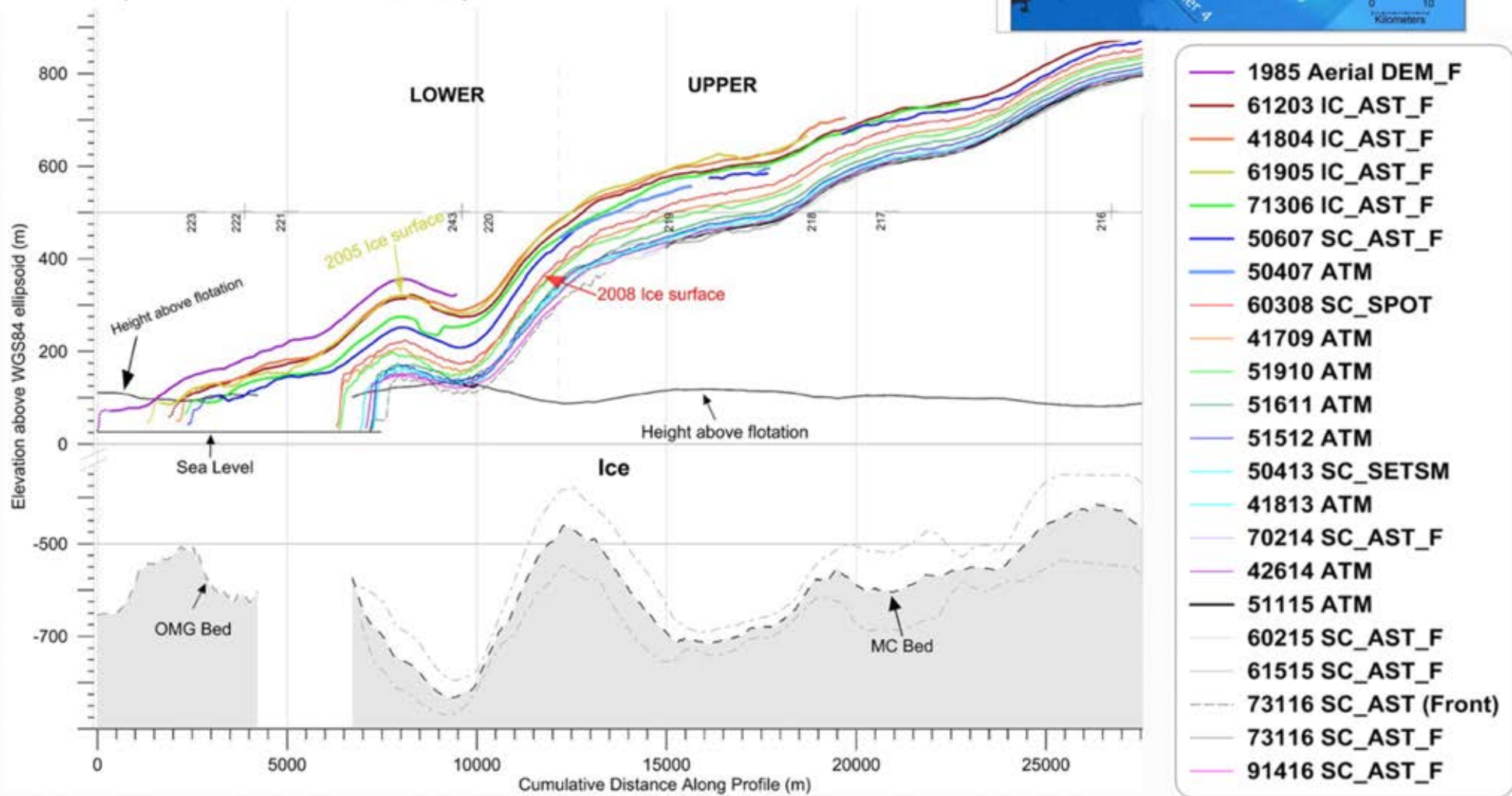
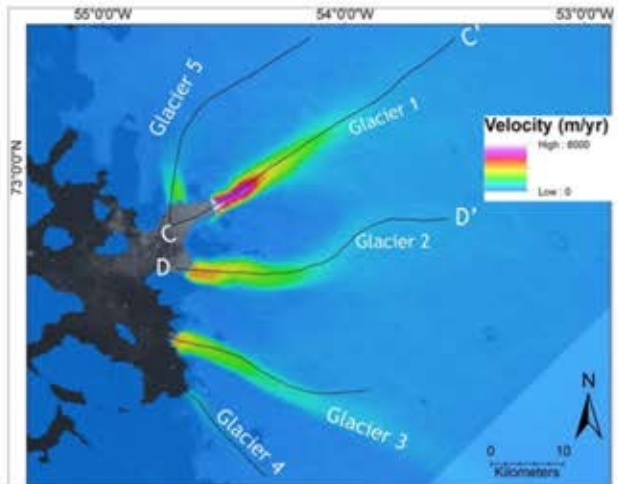
Subglacial lake drainage detected by ICESat



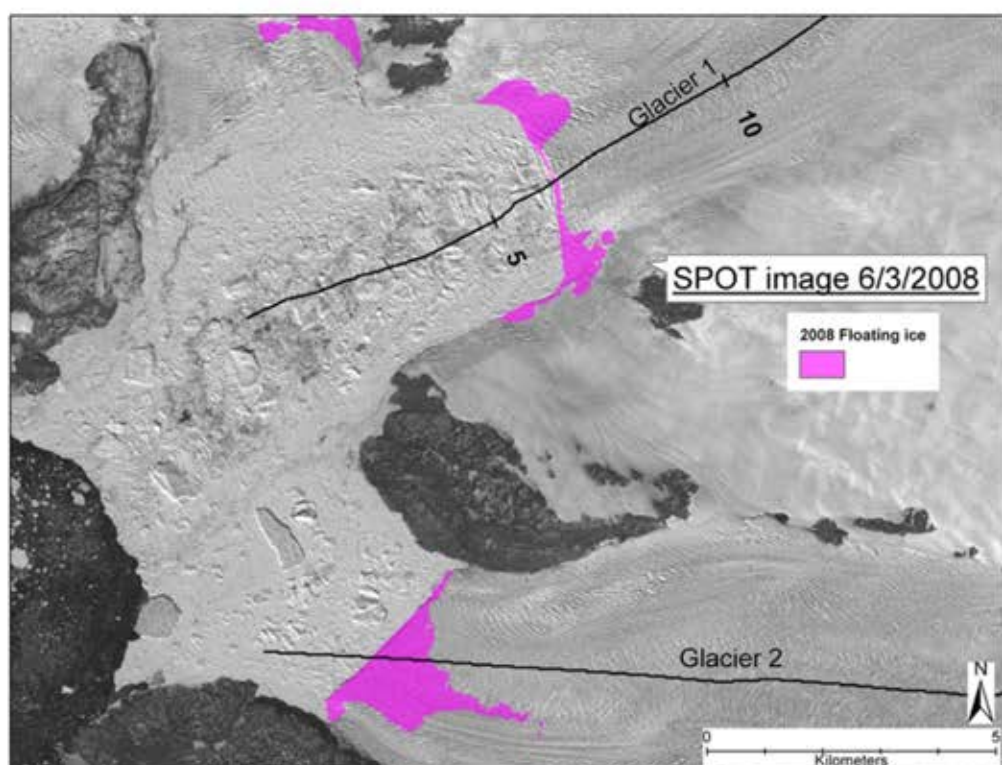
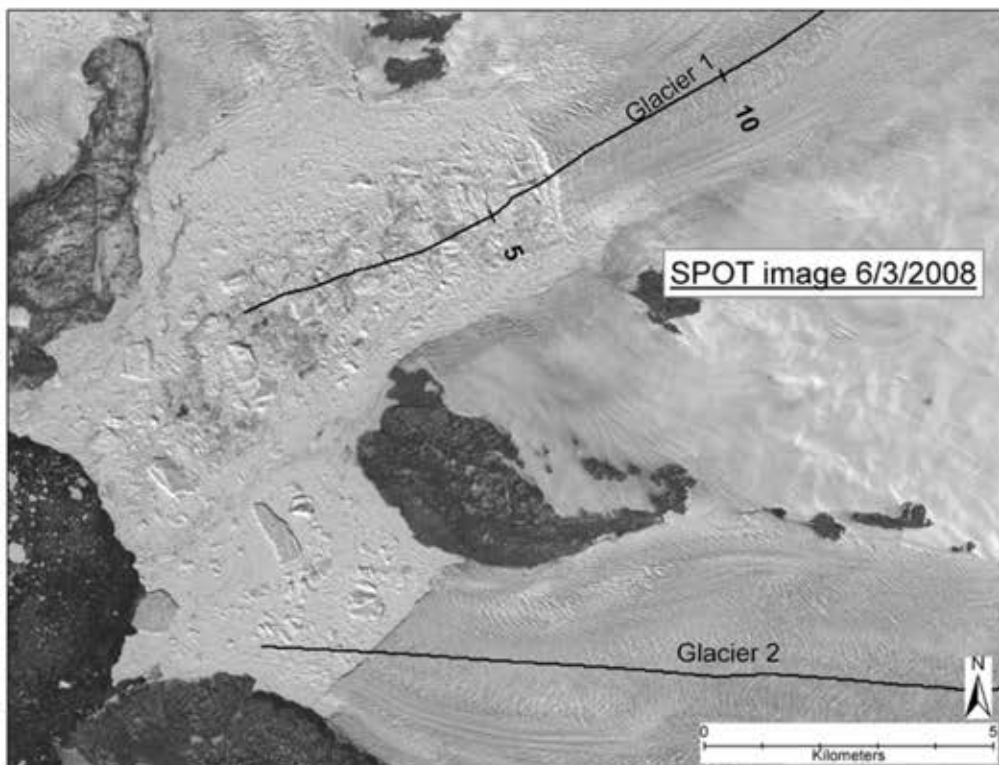
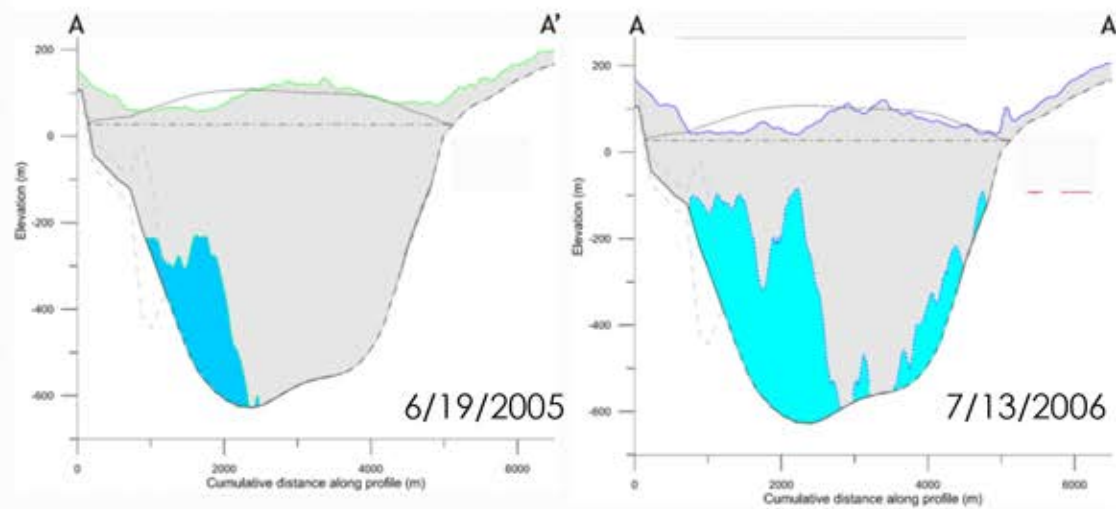
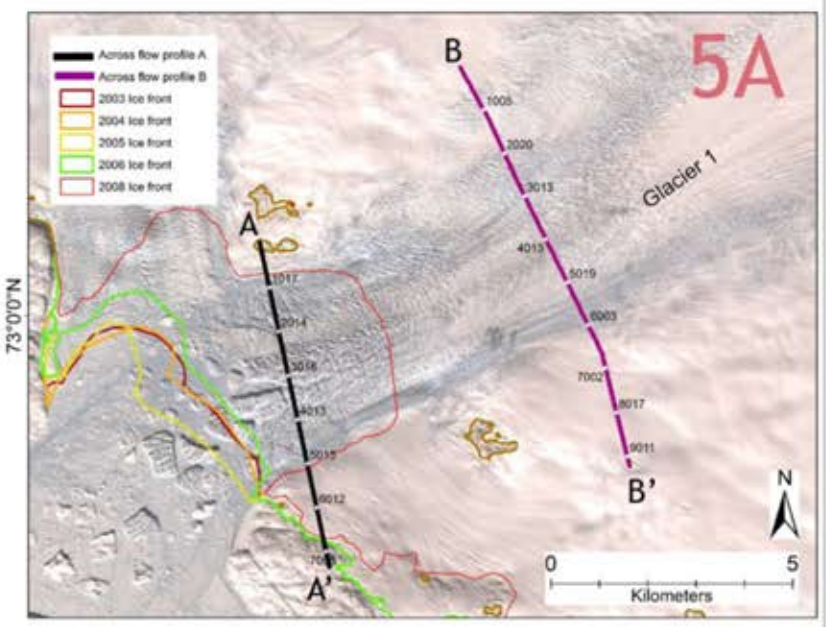
# Rapid thinning of grounded “tongue” of Upernivik Glacier 1

$dh(1985-2005) \approx 50 \text{ m}$   $dh(2005-2006) \approx 50 \text{ m}$

(Wendler et al., in prep)

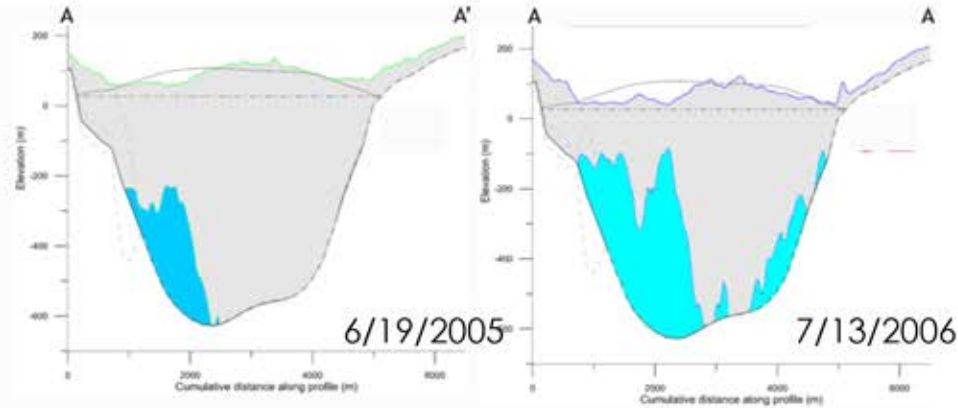


## Stable glacier centerline and evolution of floating along margins

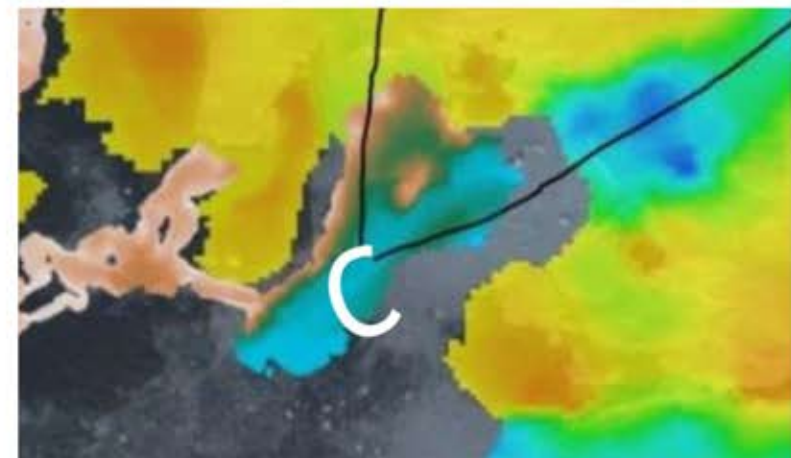
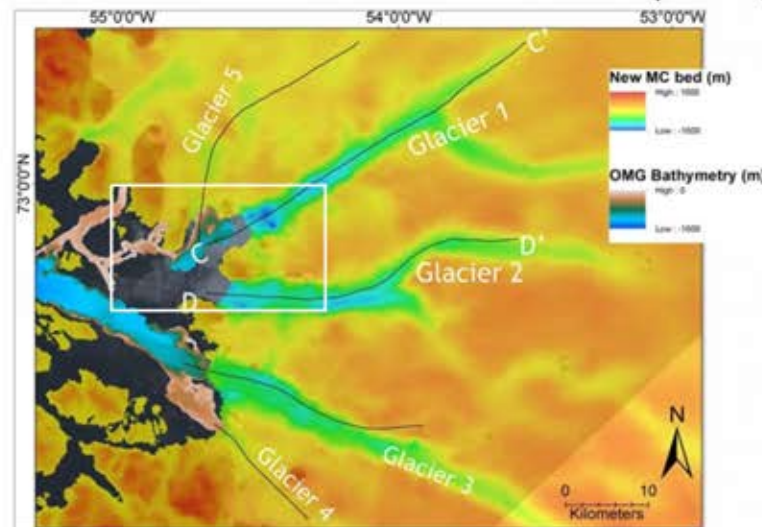


# Interpretation

- Trough along the fjord walls troughs could preferential pathways for warm, salty Atlantic waters to reach the glacier front resulting in large basal melt rates.
- Persistent positive SMB anomalies allowed a small seasonal floating tongue to persist longer into the summer season, i.e. calving off later in the season compared to normal.
- The cavity under the tongue exposed the floating ice to high basal melt rates caused by subglacial freshwater discharge-driven circulation transporting warmer ocean water into the cavity.
- Freshwater discharge is expected to be the largest at the glacier margin as meltwater reaching the bed through crevasses opened by hydrofracturing in depressions along glacier margins was flowing in the lateral troughs toward to calving front.
- The region above the terminus disintegrated once the ice was floating on both sides of the central, grounded region.



BedMachine V3 and OMG bathymetry



# Conclusions

- Land ice observations reveal long-term trends, interannual variation and spatial variability
- Ice sheet mass loss and outlet glacier thinning and retreat are broadly consistent with increasing air and ocean temperatures
- Detailed local histories indicate a complex interplay of bed geometry, ocean temperatures and subglacial geology, modulating to long-term trend of mass loss, speed-up and retreat
- More glacier histories are needed to tease out the processes!
- Close collaboration between observationists and modelers could lead to an improved understanding of land ice processes → resulting in more reliable prognosis of future ice sheet behavior

# Acknowledgements

- We thank Kurt Kjær and Niels Koorsgard (Natural History Museum, Copenhagen, Denmark) for the aerial photogrammetry DEM of Zachariæ Isstrøm, Michiel van den Broeke (University of Utrecht, Utrecht, The Netherlands) for climate data from RACMO, Sebastian Simonsen (DTU, Space, Lyngby, Denmark), and Kyle Duncan (University of Maryland, College Park, MD), David McCormick (NSOF, Suitland, MD), Carolyn Roberts, Greg Babonis (University at Buffalo, Buffalo, NY), Soroush Rezvenbehbahani (University at Kansas, Lawrence, KS) for altimetry processing and ASTER DEM correction.
- Research was funded by NASA's Cryosphere Program and NSF Office of Polar Program.

